CHARACTERIZING THE HAZARD OF RAINFALL-DIVERSE HURRICANE PROFILES IN

THE SOUTHEAST UNITED STATES

by

ALEXANDRA MUSIC

(Under the Direction of J. Marshall Shepherd)

ABSTRACT

Atlantic basin hurricanes drive serious meteorological hazards for the southeast United States, including rainfall-induced freshwater flooding. The well-known Saffir-Simpson Hurricane Wind Scale (SSHWS) communicates only wind hazard, creating the potential for low wind, high rainfall storms to be perceived as mild. Researchers have recently emphasized the need to center rainfall hazard in hurricane warning messaging. This thesis investigates the characterization of rainfall for three different Atlantic hurricanes: Florence (2018), Michael (2018), and Ian (2022). Using daily gridded gauge-based rainfall data, the distribution of rainfall is quantified, visualized, and compared between each storm. Excessive Rainfall Outlooks for each hurricane are then compared with the actual extent of flash flooding, using statistical methods for verification. Finally, the impact of rainfall and social vulnerability on FEMA disaster declarations is assessed. Results of this study assist in validating hurricane rainfall hazard communications and provide a framework for wider applications.

INDEX WORDS: Hurricanes, Precipitation, Forecast Verification, Rainfall Impacts

CHARACTERIZING THE HAZARD OF RAINFALL-DIVERSE HURRICANE PROFILES IN THE SOUTHEAST UNITED STATES

by

ALEXANDRA MUSIC

BS, Florida State University, 2022

A Thesis Submitted to the Graduate Faculty of The University of Georgia in Partial Fulfillment of the Requirements for the Degree

MASTER OF SCIENCE

ATHENS, GEORGIA

2025

© 2025

Alexandra Music

All Rights Reserved

CHARACTERIZING THE HAZARD OF RAINFALL-DIVERSE HURRICANE PROFILES IN THE SOUTHEAST UNITED STATES

by

ALEXANDRA MUSIC

Major Professor: Committee: J. Marshall Shepherd Michelle Ritchie Andrew Grundstein

Electronic Version Approved:

Ron Walcott Dean of the Graduate School The University of Georgia May 2025

ACKNOWLEDGEMENTS

I would like to thank my parents and family for always supporting my educational journey. Additionally, I would like to thank my advisor Dr. Marshall Shepherd for believing in me throughout graduate school and having an undeniable influence on me choosing to pursue a career in science communication. Thank you to all my professors, especially my committee members Dr. Michelle Ritchie and Dr. Andrew Grundstein, and to all of my educators from K-12 and beyond. Thank you to my friends, especially those in the basement of the geography building. Finally, I would like to acknowledge the role of freely available social and environmental data from the federal government, without which this thesis and countless scientific findings would not be possible.

TABLE OF CONTENTS

	Page
ACKNOWLEDGEMENTS	iv
LIST OF TABLES	vii
LIST OF FIGURES	ix
CHAPTER	
1 INTRODUCTION	1
1.1. Research Questions	6
1.2. Research Hypotheses	6
2 LITERATURE REVIEW	7
2.1. Quantifying tropical cyclone rainfall	7
2.2. Rainfall hazard communication frameworks and metrics	9
2.3. Future implications for the southeast	12
2.4. Social factors and resilience	15
3 RESEARCH DESIGN	17
3.1. Justification for selection of hurricanes	18
3.2. Data Sources and Scope	20
3.3 Methods: Research Question 1	21

	3.4. Methods: Research Question 2	22
	3.5. Methods: Research Question 3	24
4	RESULTS	20
	4.1. Hurricane Rainfall Space-Time Evolution	26
	4.2. Comparing EROs to flash flooding observations	35
	4.3. Rainfall, Social Vulnerability, and Disaster Declaration in Florence	46
5	CONCLUSION	53
REFEREN	JCFS	59

LIST OF TABLES

Pag
Table 1. Temporal scope of analysis for each storm
Table 2. Basic statistics for Florence on 9/13/18
Table 3. Basic statistics for Florence on 9/14/18.
Table 4. Basic statistics for Florence on 9/15/18
Table 5. Basic statistics for Florence on 9/16/18
Table 6. Basic statistics for Michael on 10/10/18
Table 7. Basic statistics for Ian on 9/28/22.
Table 8. Basic statistics for Ian on 9/29/22.
Table 9. Basic statistics for total rainfall data for each storm, based on the data displayed in
Figure 11
Table 10. Results of Shapiro-Wilk Normality Test
Table 11. Results of Mann-Whitney U Test
Table 12. Fractional coverage and deviation from expected values for each category of each
forecast for each day of each hurricane, for old and new ERO definitions

Table 13. FBS, WFBS, and FSS results for each hurricane under old and new ERO definition	ns. 45
Table 14. Coefficients for Rain-Only Model (green shading = significant to p < .05)	49
Table 15. p-values for Rain-Only Model (green shading = significant to p < .05)	49
Table 16. Coefficients for Rain + SVI Model	49
Table 17. p-values for Rain + SVI Model	49
Table 18. Designations vs. predicted designations for 25/100 counties.	51

LIST OF FIGURES

Page
Figure 1. 1963–2012 vs. 2013-2022 causes of death for all direct hurricane fatalities. Figure from
Brennan et al. 2023
Figure 2. Tracks of Hurricane Florence, Hurricane Michael, and Hurricane Ian over the southeast
United States. Data from HURDAT2 (NHC)
Figure 3. Annual average percentage of hurricane-season rainfall arising from tropical cyclones.
Figure from Knight & Davis, 2007
Figure 4. Example Day 2 ERO, issued on 2/23/22 and valid between 2/24/22 and 2/25/22. (WPC,
2024)11
Figure 5. Global and regional changes in storm characteristics. Note the information on TCs:
Increase in strength, decreased/unchanged cyclogenesis, slower motion in southeast United
States. Figure from IPCC WG1 report 2023, p. 1586
Figure 6. The percentage of population falling below 150% of poverty line by county in the
southeast in 2020. Data from CDC/ATSDR Social Vulnerability Index 2020 (CDC/ATSDR
2020)
Figure 7. Rainfall Totals for Hurricanes Florence, Michael, and Ian as reported in NHC Tropical
Cyclone Reports. Figures from Stewart & Berg (2019), Beven II et al. (2019), and Bucci et al.
(2023)

Figure 8. Daily rainfall for Hurricane Florence per .25 degree ² pixel with recorded rainfall 20
Figure 9. Daily rainfall for Hurricane Michael per .25 degree ² pixel with recorded rainfall 29
Figure 10. Daily rainfall for Hurricane Ian per .25 degree ² pixel with recorded rainfall 30
Figure 11. Total average hurricane-induced rainfall for hurricanes Florence, Michael, and Ian
within space/time scope of study per .25 degree ² pixel
Figure 12. Excessive Rainfall Outlooks for Hurricane Florence compared to Stage IV rainfall
flash flood proxy – 9/13/18
Figure 13. Excessive Rainfall Outlooks for Hurricane Florence compared to Stage IV rainfall
flash flood proxy – 9/14/18
Figure 14. Excessive Rainfall Outlooks for Hurricane Florence compared to Stage IV rainfall
flash flood proxy – 9/15/18
Figure 15. Excessive Rainfall Outlooks for Hurricane Florence compared to Stage IV rainfall
flash flood proxy – 9/16/18
Figure 16. Excessive Rainfall Outlooks for Hurricane Michael compared to Stage IV rainfall
flash flood proxy – 10/10/18
Figure 17. Excessive Rainfall Outlooks for Hurricane Ian compared to Stage IV rainfall flash
flood proxy – 9/28/22
Figure 18. Excessive Rainfall Outlooks for Hurricane Ian compared to Stage IV rainfall flash
flood proxy – 9/29/22

Figure 19. Comparing time/accuracy evolution of EROs between old/new ranges (positive
values=underestimation, negative=overestimation) (note that ranges differ per hurricane) 43
Figure 20. FEMA disaster declarations in North Carolina after Hurricane Florence
Figure 21. Florence total rainfall and social vulnerability factors by county. Rainfall from CPC-
Unified dataset, social data from SVI (2018)
Figure 22. ERO forecast verification for Hurricane Helene (2024) as seen in the Tropical
Cyclone Report by Hagen et al. 2025 56

CHAPTER 1

INTRODUCTION

Tropical cyclones—the strongest of which known as "hurricanes" in the United States are drivers of multiple meteorological hazards. These hazards include rainfall-induced flooding, storm surge, high winds, and tornadoes. In the United States, hurricane intensity is often communicated using the Saffir-Simpson Hurricane Wind Scale (SSHWS) (Schott et al. 2012). This scale classifies tropical cyclones (TCs) as tropical depressions, tropical storms, or hurricanes, which are additionally specified as category one, two, three, four, or five. These categories are based solely on wind speed and do not take other hazards into account. While wind intensity can be representative of a hurricane's overall threat, researchers are beginning to note the inadequacy of only considering wind in the communication of anticipated hazard (Alipour et al. 2022; Bosma et al. 2020; Camelo & Mayo, 2021; Song et al. 2020). Furthermore, wind was only responsible for about 8% of direct hurricane fatalities between 1963-2012 (Rappaport, 2014). The same study reports that 90% of these fatalities occurred in water-related incidents, with about 27% being directly attributed to rainfall. Recent data from the National Hurricane Center indicates that rainfall fatalities have overtaken storm surge fatalities in recent years, claiming 57% versus 11% of direct deaths between 2013 and 2022 (Brennan et al. 2023).

Hazard	% of direct fatalities from this cause (1963–2012)	% of direct fatalities from this cause (2013–2022)
Storm Surge	49%	11%
Freshwater Flooding	27%	57%
Wind	8%	12%
Surf/Rip Currents	6%	15%
Offshore Marine Incidents	6%	3%
Tornadoes	3%	2%
Other	1%	1%

Figure 1: 1963–2012 vs. 2013-2022 causes of death for all direct hurricane fatalities. Figure from Brennan et al. 2023.

Excluding extreme rainfall hazard from the hurricane intensity metric most widely understood by the public leaves room for misinterpretation. Many would perceive a "weaker" hurricane on the SSHWS to be minimally life-threatening, though this wind classification does not necessarily align with other hazards. For example, one can note Hurricane Harvey of 2017. This storm made landfall in Texas as a major hurricane, but quickly weakened to a tropical storm (Blake & Zelinsky, 2018). For days, the storm stalled inland near the Gulf coast of Texas, bringing unprecedented rainfall that amounted to a 9000-year flood in certain neighborhoods (Oldenborgh et al. 2017). There was a total of 65 deaths directly attributed to freshwater flooding (Blake & Zelinsky, 2018). The majority of these impacts occurred when Harvey was "weak" by the parameters of the SSHWS.

More recently, Hurricane Helene's impact in southern Appalachia in 2024 shows the importance of warning for potential rainfall impacts. By the time extreme rainfall occurred, the storm was a weak tropical cyclone and undergoing extratropical transition (Halverson &

Livingston, 2025). The areas most impacted were far from any coast and the populations of the most impacted areas were largely unprepared for extreme hurricane-related flooding. The death toll currently stands at 219 and represents the largest loss of life from a U.S. hurricane since Katrina in 2005. Though Helene is a great example of a hurricane event with extreme rainfall in the southeast, it too recently occurred for there to be sufficient literature and data for further analysis.

Nonetheless, hurricanes with extreme rainfall have occurred in the southeast in the near past. Hurricane Florence of 2018 made landfall over North Carolina as a category one storm and was soon downgraded to a tropical storm after landfall (Stewart & Berg, 2019). In a similar way to Harvey, Florence slowed upon landfall, allowing precipitation to accumulate over days. Once again, the main hazard of this hurricane was rainfall, not wind. The storm brought catastrophic freshwater flooding to the region, taking dozens of lives and requiring thousands to be rescued from flood waters. Damage throughout the region amounted to around 24 billion dollars and rivaled the statistics of many wind-intense hurricanes.

While rainfall can be an underestimated hurricane hazard, it is not always the main hazard. In 2018, Hurricane Michael caused significant damage and casualties in the Florida Panhandle as a result of storm surge and heavy winds (Beven II et al. 2019). Very few of these impacts have been attributed to rainfall. Often, rainfall hazards can vary spatially and throughout the duration of the storm. Hurricane Ian of 2022 brought hazardous heavy rainfall to the inland areas of central Florida, but its impacts in southwest Florida were mostly a result of its devastating storm surge and heavy wind (Bucci et al. 2023). Much like with wind hazards, rainfall hazards vary from hurricane to hurricane, and within hurricanes over space and time. This diversity of impact should be evaluated accordingly.

This thesis will investigate the diversity of the rainfall hazard for hurricanes making landfall in the southeastern United States. I will consider three tropical cyclones as case studies: the aforementioned hurricanes Florence (2018), Michael (2018), and Ian (2022). The rainfall from these storms will be compared spatially and temporally using spatial analytical techniques within QGIS software and evaluated for statistical significance. Next, the flash flooding outcomes will be validated against Excessive Rainfall Outlooks issued at Days 1, 2, and 3 before each day of the storm. Maps will be produced and fractional coverage will be determined using QGIS, and fractional skill scores will be calculated in R to assess the accuracy of the EROs for each storm. Finally, I will look at Hurricane Florence as a case study to determine how rainfall and social vulnerability factors played a role in determining FEMA disaster declarations during a high rainfall impact storm. This will involve creating multinomial logistic regression models in R and evaluating the significance of each variable.

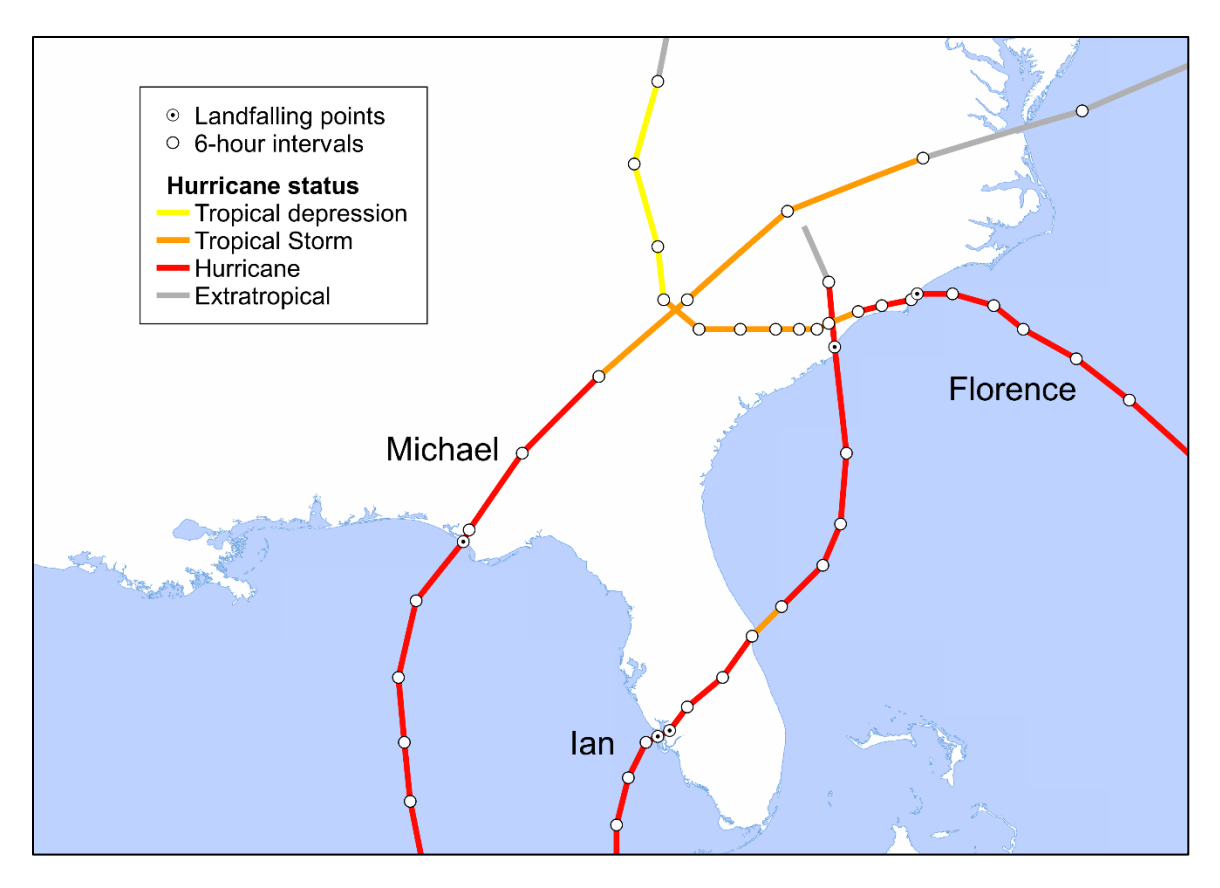


Figure 2. Tracks of Hurricane Florence, Hurricane Michael, and Hurricane Ian over the southeast United States. Data from HURDAT2 (NHC).

Results will determine the extent to which Florence, Michael, and Ian represent a spectrum of rainfall diversity. Though rainfall diversity will be defined on a relative scale for this study, the framework will be applicable to future research at larger scales. For example, researchers may categorize all known Atlantic hurricanes on a scale of rainfall diversity using similar methods. Additionally, this work will supplement the discussion of improving the communication of rainfall hazard associated with tropical cyclones. Based on a review of literature, Excessive Rainfall Outlooks have not yet been thoroughly validated in the context of tropical cyclones, and moreover have not been evaluated for rainfall-diverse TC scenarios. This thesis aims to contribute to a growing body of research that is working to improve how rainfall is integrated into hurricane warnings, which can lead to saving lives, infrastructure, and property.

This is especially important in the context of climate change, which many researchers believe is increasing the intensity of tropical cyclones and potentially lowering their translational speeds (Bender et al. 2010; IPCC, 2023; Wehner & Kossin, 2024).

1.1. Research Questions

- 1. What are the space-time rainfall distributions of Florence, Michael, and Ian, and how can we characterize each?
- 2. Do Excessive Rainfall Outlooks adequately capture diverse hurricane rainfall hazard?
- 3. For high rainfall impact hurricanes, how do county-level rainfall totals and social vulnerability factors contribute to FEMA disaster declarations?

1.2. Research Hypotheses

- 1. The space-time rainfall distributions of Florence, Michael, and Ian will differ, indicating that average daily rainfall between landfall and extratropical transition can be used to establish a scale of rainfall diversity.
- 2. Excessive Rainfall Outlooks and flash flood warnings will evolve similarly over space and time. Day 3 EROs will be sufficiently accurate when compared to flash flood observations for all rainfall scenarios; accuracy will not improve significantly for Day 2 and Day 1 EROs. Additionally, the new ERO definition will be more accurate than the old ERO definition.
- Rainfall will play a significant role in determining how a county is designated for disaster relief. Some social vulnerability factors will contribute to designation, while others will not.

CHAPTER 2

LITERATURE REVIEW

2.1. Quantifying tropical cyclone rainfall

As a foundation for understanding how hurricane rainfall hazard can be characterized, this section will provide a review of the meteorological and climatological qualities of TC rainfall. The Atlantic hurricane season occurs from June through November, but TCs can sometimes spawn outside of this period (Knight & Davis, 2007). TC rainfall has been shown to be a significant contributor of seasonal precipitation to the southeast United States, which can be seen in Figure 3 (Knight & Davis, 2009; Mazza & Chen, 2023; Shepherd et al. 2007). On the East Coast, this share is most pronounced in North Carolina and northeast Florida (Mazza & Chen, 2023). Additionally, Knight & Davis (2009) documented that the contribution of TC rainfall to total precipitation in the coastal southeast has been growing 5-10% each decade since the mid-20th century. It has been suggested that warmer sea surface temperatures in the Atlantic and Gulf of Mexico are creating wetter hurricanes, resulting in the increase in their contribution to total precipitation.

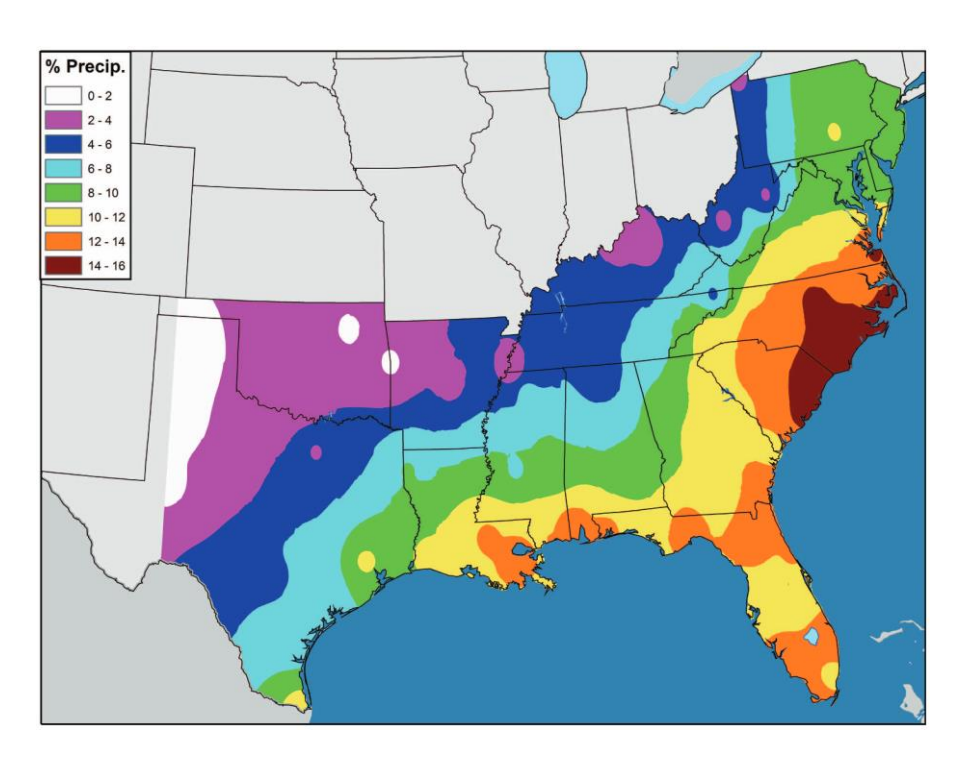


Figure 3. Annual average percentage of hurricane-season rainfall arising from tropical cyclones. Figure from Knight & Davis, 2007.

Rainfall from hurricanes can be measured by gauge stations, weather radars, and/or satellite/remote sensing (Li et al. 2020; Mazza & Chen, 2023). Each of these methods has its own advantages and disadvantages. Gauge is considered the most direct measurement, but it is still subject to error due to splash-out from heavy rain, wind interference, and low sensitivity for light rain, with the first two issues being particularly important to consider during hurricane conditions (Li et al. 2020). Additionally, there will always be spatial uncertainty with gauge-based measurements due to the need for interpolation between stations. Radars allow for more spatially and temporally continuous measurements and a wider coverage of area. However, they are subject to errors with calibration and uncertainty of observations. Radar coverage is also discontinuous in certain areas of the United States. Agreement on radar accuracy during hurricanes is inconsistent, with some case studies showing significant underestimation of rainfall and others suggesting overall adequacy (Cao et al. 2018; Medlin et al. 2007). Finally, remote

sensing has emerged as an increasingly critical component of TC rainfall calculation, allowing for global coverage and resolution that improves as technological capability improves. This method has similar disadvantages to radar by the nature of it being an indirect measurement. Studies agree that satellite remote sensing often underestimates high rates of rainfall, implying lower reliability during hurricanes (Li et al. 2020, Mazza & Chen, 2023).

2.2. Rainfall hazard communication frameworks and metrics

As discussed in Section 1, the Saffir-Simpson Hurricane Wind Scale (SSHWS) has become perhaps the most recognizable metric for discussing hurricane intensity in the United States. A former version of the SSHWS included considerations for storm surge and central atmospheric pressure (Schott et al. 2012). In 2009, the scale was modified to instead focus solely on wind, since this extra category could result in two hurricanes with the same wind speed having very different labels because pressure, like rainfall, is not always correlated with wind intensity. This decision was made in hopes of improving public interpretation and the scientific consistency of the scale. However, many researchers have criticized this simplification, stating that public perception of hurricane danger can be incomplete if the other hazards are not properly communicated alongside the SSHWS category (Alipour et al. 2022; Bosma et al. 2020; Camelo & Mayo, 2021; Song et al. 2020).

In recent years, numerous metrics have been proposed for communicating TC rainfall hazard. Going back to 2006, Senkbeil & Sheridan proposed a post-landfall hurricane classification system. This was in response to shortcomings in the SSHWS for capturing hurricane impacts over land. The Extreme Rain Multiplier (ERM), defined by Bosma et al.

(2020), is based on research that reveals the importance of "anchoring" the perception of risk in hurricane messaging. When people have a preconceived mental image of the outcome of a risk, they are more likely to take it seriously (Rickard et al. 2017). In the ERM's case, this baseline is rainfall with a local 2-year recurrence interval, which is something that most people will have experienced during their lifetime. A message that rainfall will likely be, for example, three times more extreme than a 2-year storm allows people to visualize the hazard based on past experiences, which can be more impactful to preparedness decisions than simply saying an amount of rainfall. Alipour et al. (2022) proposes the Multivariate Hurricane Index (MHI), which categorizes a hurricane as category one through five based on estimated rainfall, storm surge, and wind speed. This approach was shown to result in the categories being more correlated with damage outcomes than by following the typical wind-only framework of the SSHWS. Though many of these metrics have been introduced and still remain in the early stages of validation, they are a testament to growing scientific dissatisfaction with our current approach to TC rainfall risk communication.

There are a number of products used operationally to convey forecasts for TC rainfall, though none of them are a standard tool in the way that SSHWS has become the standard for communicating TC wind hazard, and none of them are used exclusively for TCs. The NOAA Weather Prediction Center regularly publishes a Quantitative Precipitation Forecast (QPF) (WPC, 2024). This forecast simply provides audiences with a numerical estimate of rainfall (ex: "one inch of rain."). On one hand, the QPF is quantitative and informative, but on the other hand, it does not convey any inherent concern about the hazard. Moreover, "one inch of rain" means something different throughout the landscape of a location, with flooding changing in likelihood from high-risk to low-risk areas. Recurrence intervals (i.e. "100-year storm") allow for audiences

to conceive danger in a way that is anchored in location, but this language can be problematic due to public misconceptions of statistics (Bosma et al. 2020). For example, many would take the phrase "100-year storm" to mean that it occurs every 100 years, when it is more accurate to say it has a 1% chance of occurring any given year.

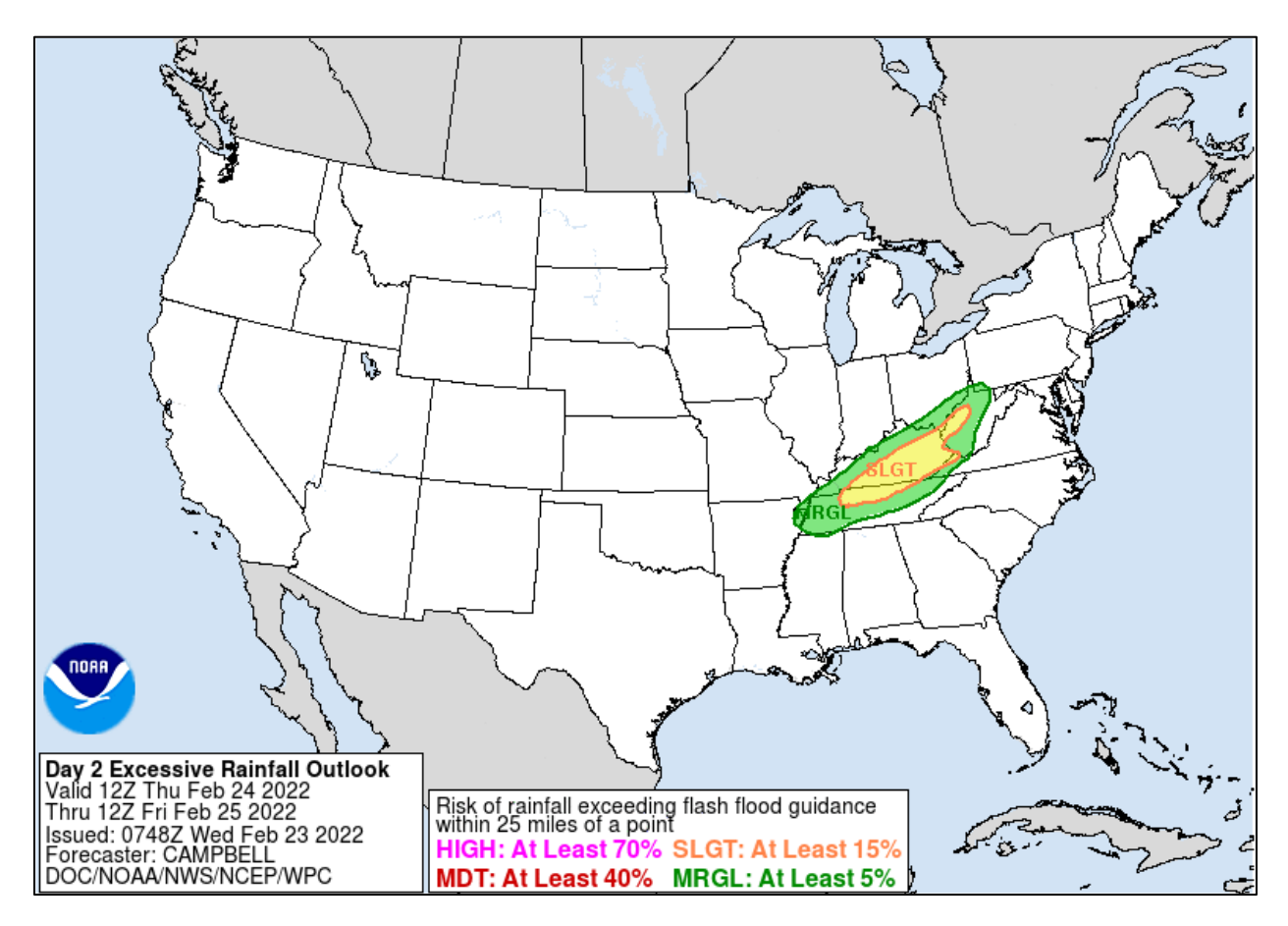


Figure 4. Example Day 2 ERO, issued on 2/23/22 and valid between 2/24/22 and 2/25/22.

(WPC, 2024)

A more effective way of communicating rainfall hazard is to focus on the hazard itself—the risk of flooding. River Forecast Centers of the United States publish flash flood guidances (FFGs) which specify the amount of rainfall needed to produce flash flooding in an area over 1, 3, or 6 hours (WPC, 2024). This is determined by assessing factors like ground moisture content, current stream level conditions, and predecessor rain events (PREs) in the region. The Weather

Prediction Center then combines these FFGs with rainfall forecasts to create an accessible national graphic known as the Excessive Rainfall Outlook (ERO). EROs depict color-coded contours over the United States that express the likelihood of flash flooding within 25 miles of a given point for day 1 (approximately the next 24 hours), day 2 (the following 24 hours), and so on up to day 5 in advance of a rainfall event. These contours specify whether the likelihood of FFG exceedance is either marginal (>5%), slight (>15%), moderate (>40%), or high (>70%) (WPC, 2024). Each of these categories was redefined in early 2022 to reflect increased confidence in the ERO as a result of verification efforts (Vallee, 2022). Before this change, marginal was 5-10%, slight was 10-20%, moderate was 20-50%, and high was >50%. Figure 4 shows an example of an ERO using the current categories. Note that this figure depicts a day 2 outlook, issued on 2/23/22 and therefore depicting forecasts for the period 2/24/22 12Z to 2/25/22 12Z.

2.3. Future implications for the southeast

As discussed in Section 2.1, the share of annual rainfall in the southeast that is owed to hurricanes is becoming more prominent (Knight & Davis, 2009; Mazza & Chen, 2023). The Intergovernmental Panel on Climate Change (IPCC) states in their AR6 report that they have high confidence that rainfall associated with hurricanes is increasing, and that this precipitation will increase by up to 28% under a high 4°C warming scenario (IPCC, 2023). Specifically, they name anthropogenic climate change as a highly likely cause of the extreme rainfall of Hurricane Harvey (2017), stating that this has likely been true for other rainfall-intense hurricanes as well. The IPCC has medium confidence that the movement of TCs over the continental United States is slowing, increasing the hazard duration of rainfall. This is potentially demonstrated by the

spatially lingering nature of hurricanes Harvey and Florence leading to severe flooding (Reed et al. 2020). Additionally, there is medium-high confidence that the proportion of intense hurricanes to less intense hurricanes is being augmented by climate change. (IPCC, 2023) Some of these outlooks are shown below in Figure 5, taken from the IPCC's 2023 Working Group 1 (WG1) report.

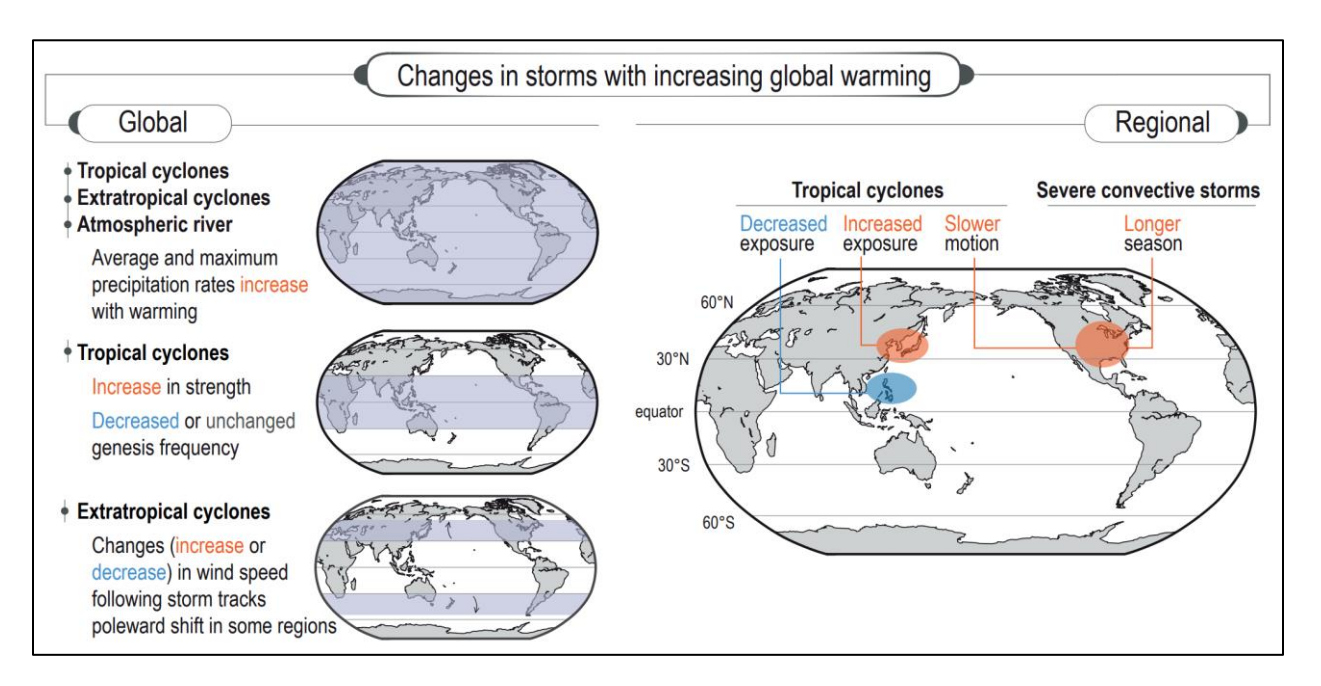


Figure 5. Global and regional changes in storm characteristics. Note the information on TCs: Increase in strength, decreased/unchanged cyclogenesis, slower motion in southeast United States. Figure from IPCC WG1 report 2023, p. 1586.

Climate risk is considered a function of hazard, exposure, and vulnerability (IPCC, 2023; KC et al. 2021). Rainfall hazard is not the only component of climate risk that is increasing in the southeast. Demographic shifts to hurricane-prone areas are resulting in higher exposure to TC rainfall hazard, with exposure being a key aspect of overall climate risk (Swain et al. 2020). Combined with the future TC trends in Figure 5 owed to global climate change, it is evident that both hazard and exposure are becoming enhanced. The third aspect of risk, vulnerability, is also

something that is very prevalent in the southeast. Figure 6 shows the distribution by county of one vulnerability factor, poverty, across the southeast (CDC/ATSDR 2020). Visual analysis reveals that poverty becomes more pronounced just inland from the coast. Because TC rainfall can be an inland hazard (not just coastal, like with storm surge), this is important to consider when determining the overall risk brought on by rainfall-induced flooding during hurricanes.

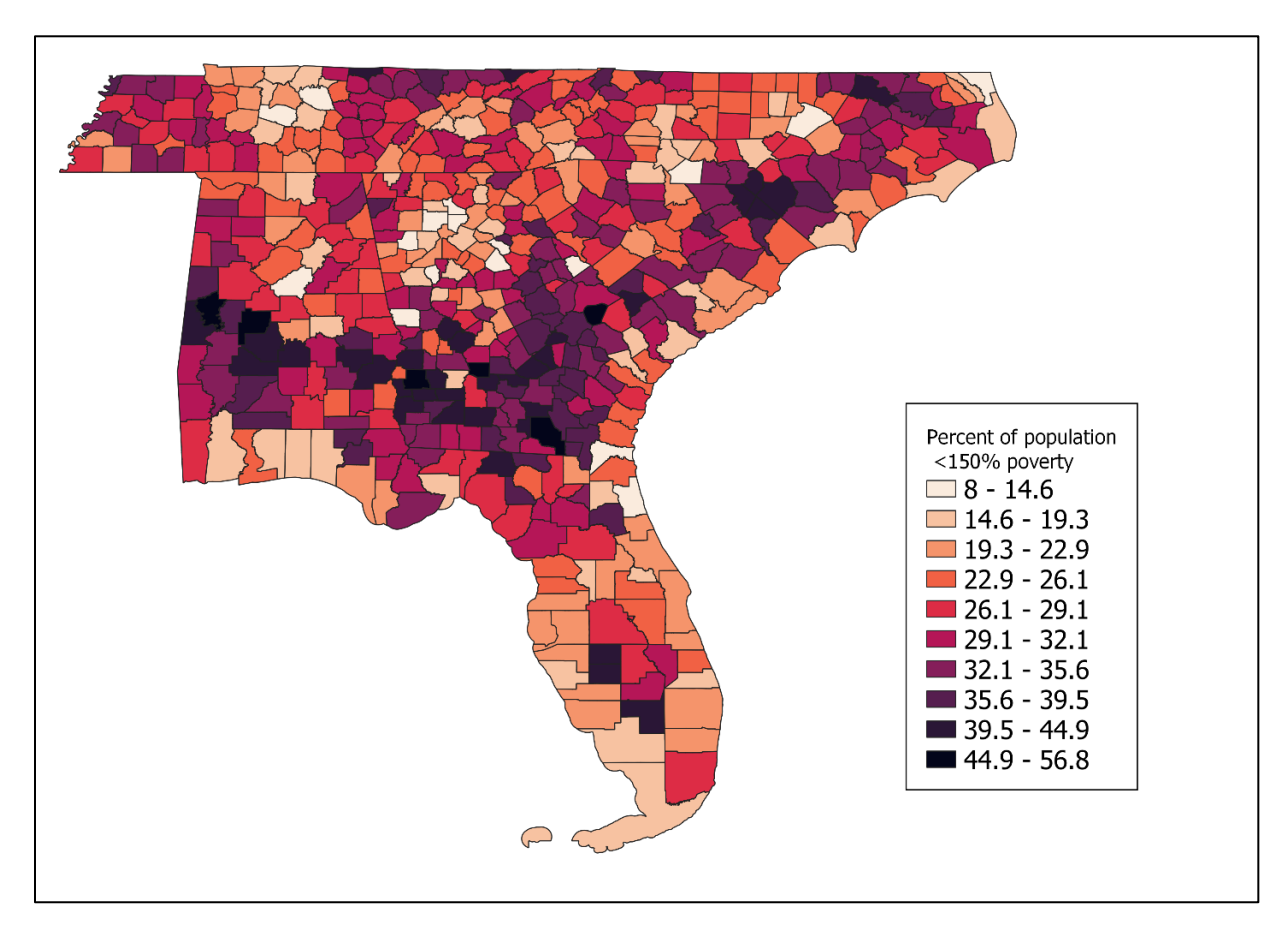


Figure 6. The percentage of population falling below 150% of poverty line by county in the southeast in 2020. Data from CDC/ATSDR Social Vulnerability Index 2020 (CDC/ATSDR 2020).

When assessing all three factors of hazard, exposure, and vulnerability, it is clear that future conditions in the southeast United States will become more favorable for creating devastating consequences for TC rainfall. This emphasizes the importance of venturing to better

characterize rainfall diversity of hurricanes in order to improve communication and mitigate the impacts of these future conditions.

2.4. Social factors and resilience

As shown in Figure 6, counties across the southeast vary significantly in poverty rates. Variation at the county level also occurs throughout this region with other social factors, such as unemployment, uninsurance, income level, and mobile home usage (CDC/ATSDR 2020). These factors are important to consider as they should directly determine, in tandem with the degree of the hazard, what time of assistance is needed after a natural disaster like a hurricane. A fairly wealthy county, for example, might require less public assistance after extreme rainfall than a county with less sufficient infrastructure.

In the U.S, FEMA keeps records of county-level federal assistance designations after major disasters (FEMA 2024). Governors and Tribal Chief Executives are responsible for specifying which types of federal assistance programs to request. This assistance can come in the form of individual assistance (crisis counseling, unemployment assistance, etc), and/or public assistance, which is broken up into seven categories (A-G) which designate debris removal, emergency protective measures, roads and bridges, water control facilities, buildings and equipment, utilities, and parks and recreation, respectively. For determining the activation of individual assistance, FEMA considers demographic factors of the disaster-affected population along with other variables like uninsured homes impacted and casualties. For public assistance, FEMA takes into account cost, localized impacts, compounding hazards, and more. It should be noted that federal approval of disaster declaration requests is not always unbiased. Political party

affiliation and upcoming elections have been shown to impact assistance approval rates (Husted & Nickerson 2014). This demonstrates the need for a more objective process of distributing federal disaster assistance, which this thesis will further address.

CHAPTER 3

RESEARCH DESIGN

To investigate the variability of tropical cyclone rainfall hazard, this thesis project will compare the rainfall profiles of Hurricane Florence (2018), Hurricane Michael (2018), and Hurricane Ian (2022). Based on background research discussed in Section 1, the rainfall profiles of these hurricanes seem to differ significantly. This case study approach will allow for an indepth assessment of the utility of framing rainfall hazard as a unique component of hurricane hazard. With the exception of Research Question 3, each hurricane mentioned will be considered when answering the following research questions:

Research Question 1: What are the space-time rainfall distributions of Florence, Michael, and Ian, and how can we characterize each?

Research Question 2: Do Excessive Rainfall Outlooks and flash flood warnings adequately capture diverse rainfall hazard?

Research Question 3: For high rainfall impact hurricanes, how do county-level rainfall totals and social vulnerability factors contribute to FEMA disaster declarations?

3.1. Justification for selection of hurricanes

To select the three hurricanes for this study, this research began by narrowing down possible choices by region (must have impacted southeast U.S.), time frame (occurring between 2018 and 2022), and significance of impact (name retired from future use). Next, NHC Tropical Cyclone Reports were consulted to assess the role of rainfall in contributing to the impacts of potential hurricanes to be studied. These reports describe rainfall-related deaths and damage along with a glimpse at rainfall intensity. For the study, a high rainfall-impact hurricane, a low rainfall-impact hurricane, and a moderate rainfall-impact hurricane were to be selected.

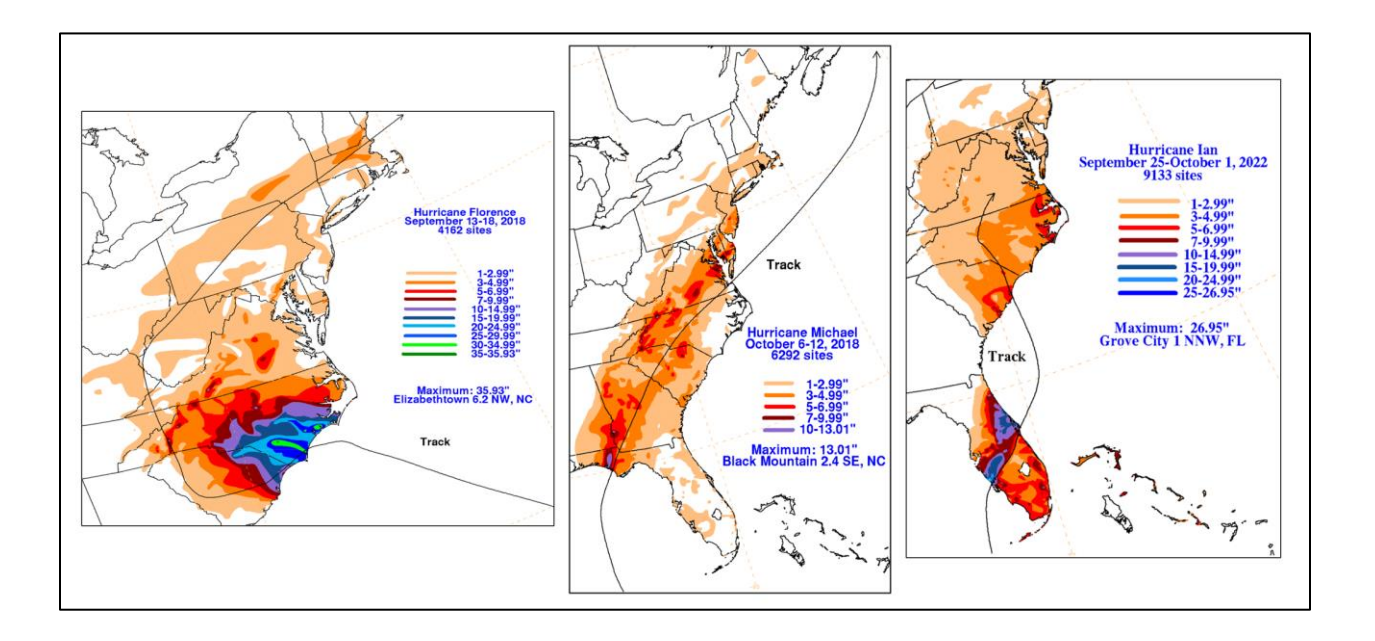


Figure 7. Rainfall Totals for Hurricanes Florence, Michael, and Ian as reported in NHC

Tropical Cyclone Reports. Figures from Stewart & Berg (2019), Beven II et al. (2019), and

Bucci et al. (2023).

Hurricane Florence (2018) immediately stuck out as a high rainfall impact hurricane in the region. With a slow forward speed after landfall, the storm lingered over the Carolinas for days, bringing extreme flash flooding to a large area as shown in Figure 7 (Stewart & Berg

2019). The vast majority of casualties were due to freshwater flooding, accounting for 17 out of 22 deaths (77.3%). Nearly 100,000 structures were flooded with many experiencing moderate or major damage. Over 5,000 individuals needed to be rescued from flood waters by boat, helicopter, or Humvee in North Carolina alone.

Occurring the same year as Hurricane Florence, Hurricane Michael had no deaths attributed to rainfall before undergoing extratropical transition (Beven II et al. 2019). Most of the damage and casualties were due to high wind and storm surge that impacted the coastal panhandle of Florida. Though rainfall was present during Michael, the relatively fast forward speed of Michael prevented rainfall from accumulating as severely as it did during Florence. In Figure 7, one can note the large rainfall swatch with a maximum occurring in North Carolina, which was measured outside of the temporal scope of this study (see Table 1).

Hurricane Ian (2022) had a moderate rainfall impact that fell between the rainfall impact of Florence and Michael according to a qualitative analysis of data discussed in its tropical cyclone report (Bucci et al. 2023). During Ian, some inland deaths were attributed to flash flooding, mostly occurring in east central Florida. There were 66 direct fatalities in total, and 12 were owed to freshwater flooding (18.2%). Most of the devastating impacts to life and property were caused by storm surge and wind, especially in coastal southwest Florida. As shown in Figure 7, high amounts of rainfall still occurred in certain areas, though not to the extent of the maxima that occurred during Florence.

3.2. Data Sources and Scope

The analysis of each hurricane will occur at daily timesteps, beginning at 12Z (UTC) immediately before continental U.S. landfall and ending at 12Z before tropical cyclone status was revoked. This is because most data at daily timesteps is organized in 12Z-12Z periods (NOAA, 2023). For Hurricane Florence, extratropical transition completed at 12Z on September 17, 2018, so analysis will end at this time rather than before (Stewart & Berg, 2019). Any rainfall occurring within a 500 km radius of interest (ROI) of the hurricane track will be included in the analysis, following the conventions of prior studies (Bosma et al. 2020). Only rainfall occurring over the continental United States will be considered.

Name	Beginning of	U.S. Landfall	End of	TC status	Days to be
	analysis		analysis	revoked	analyzed
Florence	09/13/18 12Z	09/14/18 11Z	09/17/18 12Z	9/17/18 12Z	4
Michael	10/10/18 12Z	10/10/18 17Z	10/11/18 12Z	10/12/18 0Z	1
Ian	09/28/22 12Z	09/28/22 19Z	09/30/22 12Z	10/01/22 0Z	2

Table 1. Temporal scope of analysis for each storm

For information relating to storm location, wind strength, pressure, and size, this thesis will reference the HURDAT2 database managed by the NHC, which contains data points at 6-hour intervals for Atlantic tropical cyclones (Landsea & Franklin, 2013). Rainfall measurements will be sourced from the CPC-Unified data collection and analyzed as daily totals (Xie et al. 2007). This dataset consists of gridded daily gauge-based observations at a .25x.25-degree resolution. TC-related rainfall will be identified by cropping all CPC-Unified data sets to the 500 km ROI.

To determine the spatial extent of impacts, data from the WPC's Intense Rainfall and Flash Flood Reports database will be used. In particular, this will include Stage IV rainfall

analysis of rainfall exceeding the local FFG inflated to a 40 km radius (Schmidt, 2007).

Additionally, Tropical Cyclone Reports from the NHC and NOAA's Storm Data publication will be referenced, which contain data on deaths and damage, distinguishing how each hazard contributed to overall hurricane impacts (Beven II et al. 2019; Bucci et al. 2023; Stewart & Berg, 2019). These impacts will be analyzed in the context of the CDC's Social Vulnerability Index (SVI) to determine how they are distributed across socioeconomic divides (CDC/ATSDR, 2018). Data from FEMA will provide information on disaster declaration assistance designations at the county level. Finally, images and shapefiles from the WPC's Excessive Rainfall Outlook archives at days 1, 2, and 3 in advance of each storm day will be used, due to EROs before Day 3 not being consistently available.

3.3. Methods: Research Question 1

To address the first component of the research question, a spatiotemporal analysis of rainfall patterns will be conducted for each storm. NHC's HURDAT2 data will be used to place the tracks in QGIS to define the 500 km ROI. The CPC-Unified rainfall data will then be added to the maps and clipped to only the areas contained within the ROI. Any pixels containing no rainfall will be excluded from the analysis. With the precipitation area identified, daily rainfall maps for each tropical cyclone will be produced using QGIS. This will be done for every day of every storm, which is delineated in Table 1. Additionally, total rainfall maps will be produced for each storm, with the total rainfall for each pixel over all days depicted.

Next, rainfall diversity across the three hurricanes will be assessed. This will be done by dividing the total rainfall for each hurricane (sum of all pixels) by the count of pixels with

rainfall. This is possible by using the "raster layer statistics" function in QGIS. These averages will first be compared by average, but then also assessed for differences in maximums, ranges, and standard deviation to get a sense of all the ways in which the data sets differ. At first, this comparison will take place at face value before moving to a quantitative analysis in R that also tests for significance.

In R, all three data sets, which contain measures of totals for each non-zero pixel in the ROI, will be tested for normality using a Shapiro-Wilk normality test. This test will help determine the most appropriate significance test to be used. If the data sets are normal, the two-sample t-test will be used. Otherwise, the Mann-Whitney U test, which does not assume normality, will be used. The p-values for the result of each significance test will be compared to the standard p < 0.05 threshold for determining whether differences between data sets are statistically significant.

3.4. Methods: Research Question 2

To assess how well flash flooding forecasts aligned with observed flash flooding, EROs will be assessed against a Stage IV rainfall flash flood proxy. This will be done for each Day 1, 2, and 3 issuance in advance of each day of the storm as defined in Table 1. First, this will be conducted as a visual analysis by producing maps in QGIS. Like was done with the rainfall data in Section 3.2, all flash flooding and ERO polygons will be clipped to the 500 km ROI when necessary. This will provide a visual component of the forthcoming quantitative analysis, which will be valuable as a way to verify results.

Next, using QGIS, fractional coverage will be calculated for each ERO category for each issuance for each day of each storm (e.x. Florence – 9/13/19 – Day 3 – Marginal: 2.17% covered by flash flood proxy). Though there are different methods of verification, fractional coverage was chosen due to its ability to lead to a numerical outcome that can be compared between categories, days, models, and storms. This procedure is based on a similar procedure performed in Erickson et al. 2021 for verifying ERO contours. QGIS has a function called "overlap analysis" for the purpose of calculating fractional coverage. Results will be placed in a spreadsheet and compared to expected values for the old and new ERO definitions. For instance, the expected value for the above example (as it's for Marginal) would be 5-10% for the old definition or 5% < x < 15% for the new definition. For simplicity, the new definition will be defined as a range between 5-15%, as the distinction is negligible for the purposes of this study. The difference between the forecasted range and the calculated fractional coverage will then be recorded. For a calculated fractional coverage that falls within the forecasted range, the difference is zero. If the coverage falls below the range, the difference will be coverage – (range minimum). If the coverage falls above the range, the difference will be calculated as coverage – (range maximum). These differences will be displayed on a table as well as on charts that show the evolution of the differences over time and for each hurricane.

Next, to validate the EROs, the Fractional Brier Score (FBS) and Fractional Skill score (FSS) will be calculated for each hurricane, particularly in the context of both the old and new ERO definitions. To calculate the FSS, the worst possible Fractional Brier Score (WFBS) must be calculated as it changes for each event. These scores are defined as:

FBS =
$$\frac{1}{I} \sum_{i=1}^{I} (NP_{i,f} - NP_{i,o})^2$$
,

WFBS =
$$\frac{1}{I} \left(\sum_{i=1}^{I} NP_{i,f}^{2} + \sum_{i=1}^{I} NP_{i,o}^{2} \right)$$
, and

$$FSS = 1 - \frac{FBS}{WFBS}.$$

 $NP_{i,f}$ is the forecasted fractional coverage, $NP_{i,o}$ is the observed fractional coverage, and WFBS is the worst possible FBS for the data (Zhao & Zhang 2018, Necker et al. 2024). Like with the fractional coverage differences, the difference between $NP_{i,f}$ and $NP_{i,o}$ will be zero if the fraction is within the forecasted range, otherwise subtracted by the range's maximum or minimum depending on where the observation lies. The FBS becomes more accurate as it approaches zero, but FBS scores cannot be compared between hurricanes due to differences in the definition of each. To remedy this, the FSS, a normalized form of the FBS, will be calculated. The higher the FSS result is (i.e. closer to 1), the more skillful the ERO was in predicting the spatial extent of flash flooding.

3.5. Methods: Research Question 3

Finally, a multinomial logistic regression model will be created in R to determine how rainfall and social variables may play a role in assigning a county a FEMA disaster declaration designation after a high rainfall impact hurricane. This part of the thesis will only look at Hurricane Florence, as this hurricane was undoubtedly the most costly in terms of both lives and monetary value in the realm of rainfall (Stewart & Berg 2019). This will also help disentangle

the effects of wind and storm surge from the disaster declaration process, as these two variables are outside the scope of this thesis. Data from FEMA will provide information on disaster declarations for each county in North Carolina, the main state of impact for Florence. These county polygons will be joined with SVI data, particularly with variables like mobile home percentage, per capita income, and percentage uninsured population. These variables could potentially have an impact on what kind of funding the disaster declaration accounts for, based on information from FEMA, especially for the factor of whether or not individual assistance was designated (FEMA 2024). Next, rainfall values will be sampled at the centroid of each county and joined to the county-level information to account for the physical hazard component. This factor is theoretically prerequisite to any social factors, as all counties receiving relief should have experienced rainfall to some extent.

A multinomial logistic regression model has been chosen for this part of the research as it handles categorical outcomes, which represents the data for disaster declaration designations. Other methods, such as multiple linear regression, require the outcome data to be numerical. Two models will be created to compare the roles of rainfall and social vulnerability in the process. The first model will represent the county relief designation as a function of only rainfall. This will illustrate, to an extent, how much of a role rainfall alone played in the designation. It is assumed that the relationship will be significant as rainfall was the main hazard of Florence.

Next, a multinomial logistic regression model will be created that factors in SVI variables. For this model, the accuracy will be calculated along with the significance of each SVI variable's role in predicting the result. The results for this model will be compared to the rainfall-only model to provide insight into whether or not social vulnerability was a factor in the relief provided to counties.

CHAPTER 4

RESULTS

4.1 Hurricane Rainfall Space-Time Evolution

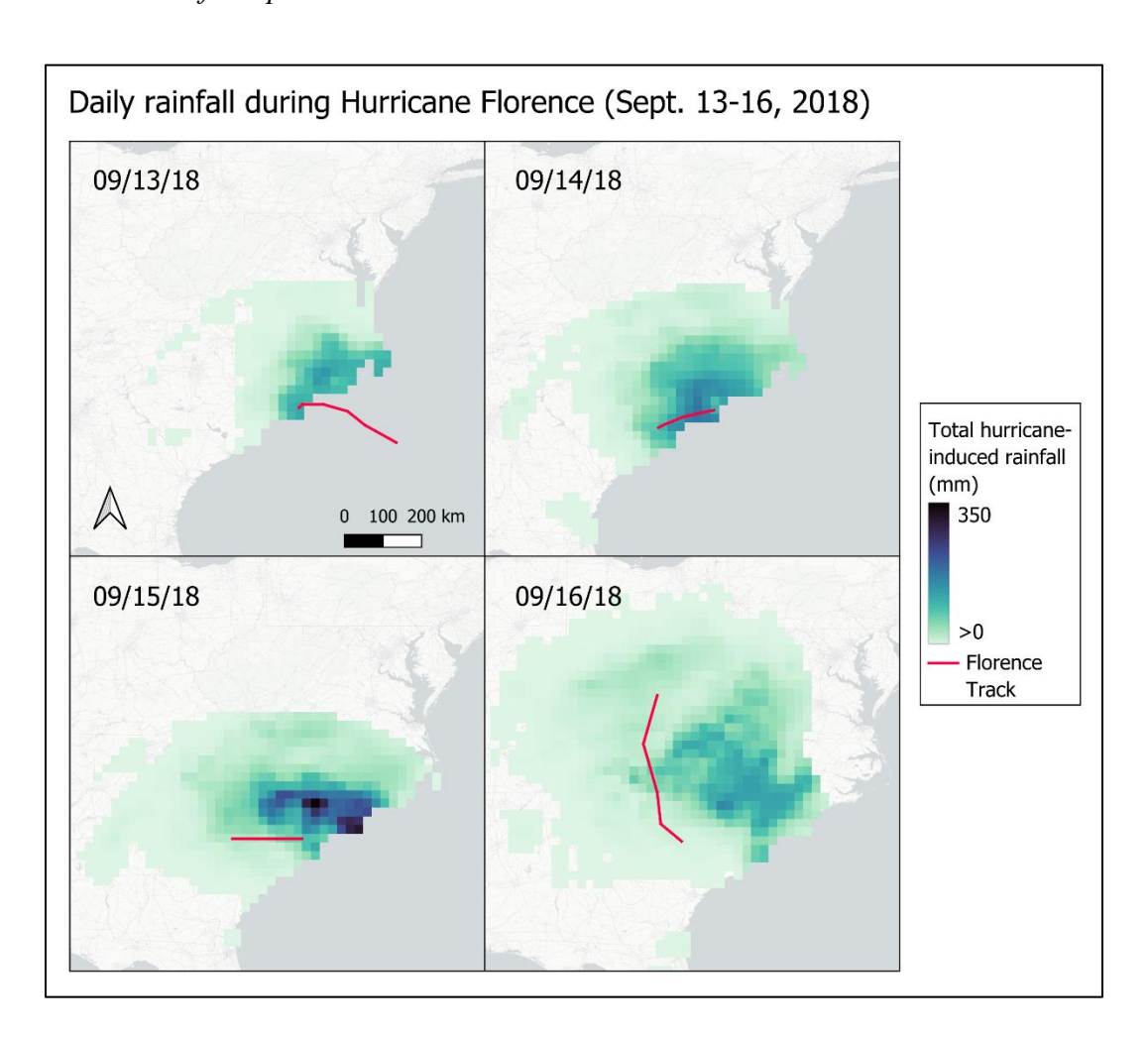


Figure 8. Daily rainfall for Hurricane Florence per .25 degree² pixel with recorded rainfall.

Hurricane Florence lasted for four days between U.S. landfall and extratropical transition. Figure 8 shows how extreme rainfall occurred each day, with maxima between 140.61 and 347.98 mm (5.54 and 13.7 in.) per day. Maxima, minima, and other basic statistical information for Florence are listed in Tables 2-5. As shown in Figure 8, rainfall tended to be prevalent around the right-front quadrant Hurricane Florence, which is considered to be the most hazardous region of a hurricane. Additionally, maxima were found in both inland and coastal areas, illustrating the idea that hurricanes should not be considered a coastal hazard alone.

The third day of Hurricane Florence, 9/15/18, is when the storm peaked for the Max, Sum, and Mean attributes. Standard deviation also peaked on this day, meaning that rainfall measurements for each pixel were the least clustered. As shown by the track on each day, Florence moved slowly inland, allowing rainfall to accumulate over time.

Pixels w/ rainfall	259
Min (mm)	0.021
Max (mm)	140.613
Range (mm)	140.592
Sum (mm)	6935.906
Mean (mm/pixel)	26.780
std_dev	38.977
sum_of_squares	391962.0356

Table 2: Basic statistics for Florence on 9/13/18.

Pixels w/ rainfall	442
Min (mm)	0.025
Max (mm)	183.417
Range (mm)	183.392
Sum (mm)	14916.250
Mean (mm/pixel)	33.747
std_dev	43.661
sum_of_squares	840655.706

Table 3: Basic statistics for Florence on 9/14/18.

Pixels w/ rainfall	573
Min (mm)	0.0212
Max (mm)	347.980
Range (mm)	347.959
Sum (mm)	21555.650
Mean (mm/pixel)	37.619
std_dev	59.667
sum_of_squares	2036438.290

Table 4: Basic statistics for Florence on 9/15/18.

Pixels w/ rainfall	1025
Min (mm)	0.021
Max (mm)	156.799
Range (mm)	156.778
Sum (mm)	24819.473
Mean (mm/pixel)	24.214
std_dev	32.913
sum_of_squares	1109255.807

Table 5: Basic statistics for Florence on 9/16/18.

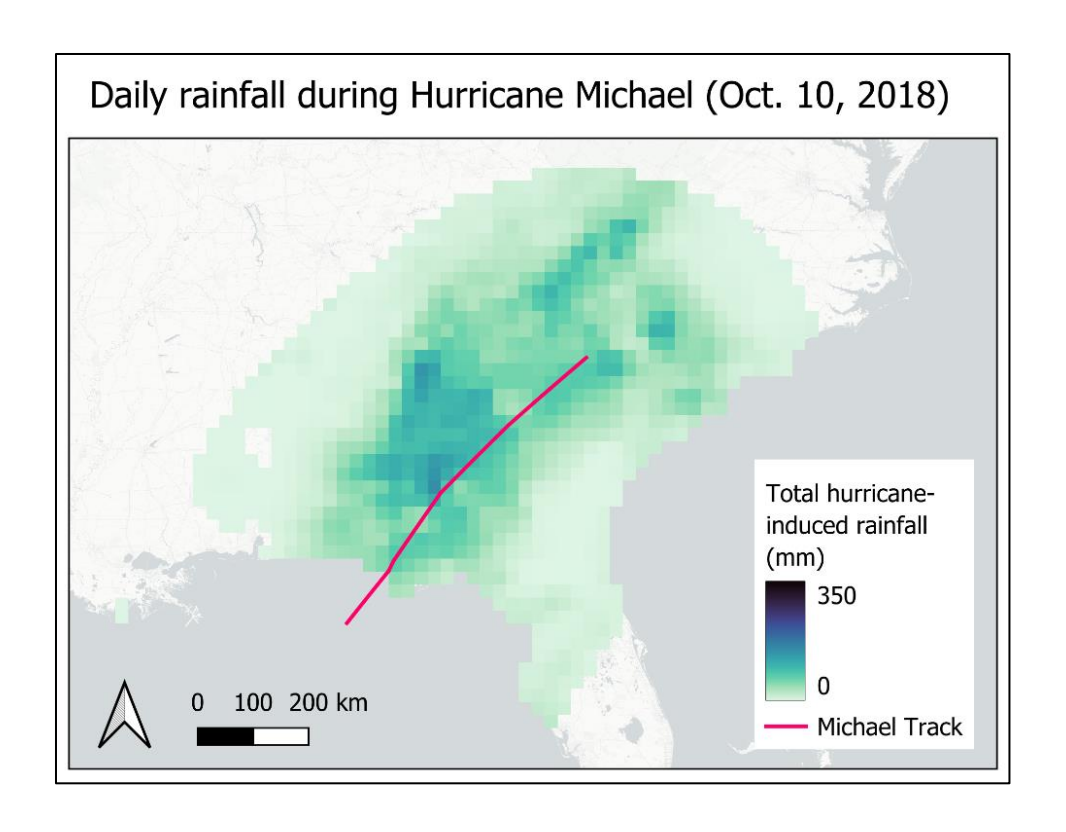


Figure 9: Daily rainfall for Hurricane Michael per .25 degree² pixel with recorded rainfall.

Hurricane Michael had the shortest period of study out of the three hurricanes chosen in this case study. Only one full day existed between landfall and extratropical transition. During this one day, there was significant clustering of rainfall around the center of the storm as seen in Figure 9, though the maximum rainfall did not reach the extremes of Florence. Max rainfall was 151.3 mm (5.96 in.), with an average of 32.23 mm (1.27 in.) per pixel. At 31.06, the standard deviation of the pixels was lower than that of any day of Florence, indicating that Michael distributed rainfall more evenly throughout the ROI. Further basic statistics for Michael are shown in Table 6.

Pixels w/ rainfall	1061
Min (mm)	0.039
Max (mm)	151.305
Range (mm)	151.266
Sum (mm)	34194.722
Mean (mm/pixel)	32.229
std_dev	31.059
sum_of_squares	1022557.217

Table 6: Basic statistics for Michael on 10/10/18.

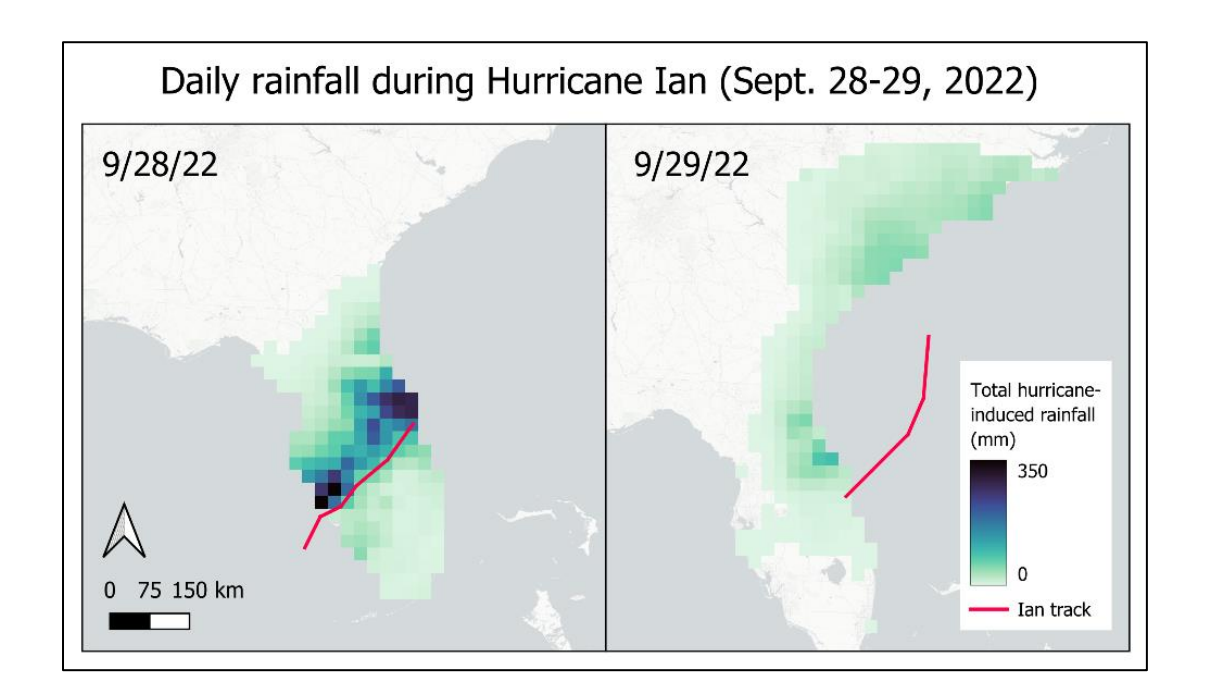


Figure 10: Daily rainfall for Hurricane Ian per .25 degree² pixel with recorded rainfall.

Hurricane Ian lasted for two days between landfall and extratropical transition. As seen in Figure 10, Ian's eye was located over the Atlantic Ocean for almost all of 9/29/22 after passing over the Florida peninsula. In the two figures, we see a stark visual difference between rainfall on the 28th and 29th. This difference is noted in the basic statistics shown below in Tables 7 and 8 as well. It should be noted that the presence of Ian over the ocean could be obscuring rainfall peaks, as the rainfall data used for this study only includes rainfall occurring over land. However,

because this rainfall at sea would not have any direct societal impacts, including this information is not necessary for the purposes of this study.

Pixels w/ rainfall	198
Min (mm)	0.026
Max (mm)	383.950
Range (mm)	383.924
Sum (mm)	11011.574
Mean (mm/pixel)	55.614
std_dev	76.053
sum_of_squares	1139458.693

Table 7: Basic statistics for Ian on 9/28/22.

Pixels w/ rainfall	268
Min (mm)	0.025
Max (mm)	92.087
Range (mm)	92.061
Sum (mm)	4618.316
Mean (mm/pixel)	17.233
std_dev	16.417
sum_of_squares	71957.313

Table 8: Basic statistics for Ian on 9/29/22.

To categorize the rainfall hazard of each storm, Equation 1 was used, where n is the total number of pixels with rainfall over the duration of the hurricane, d is the amount of days being analyzed for the storm, and $p_{i,j}$ is the amount of rainfall at pixel j on day i. This equation was applied to each storm, and results are shown in Figure 11 along with an aggregate depiction of total rainfall.

$$r = \frac{1}{n} \sum_{j=1}^{n} \sum_{i=1}^{d} p_{i,j}$$

Equation 1

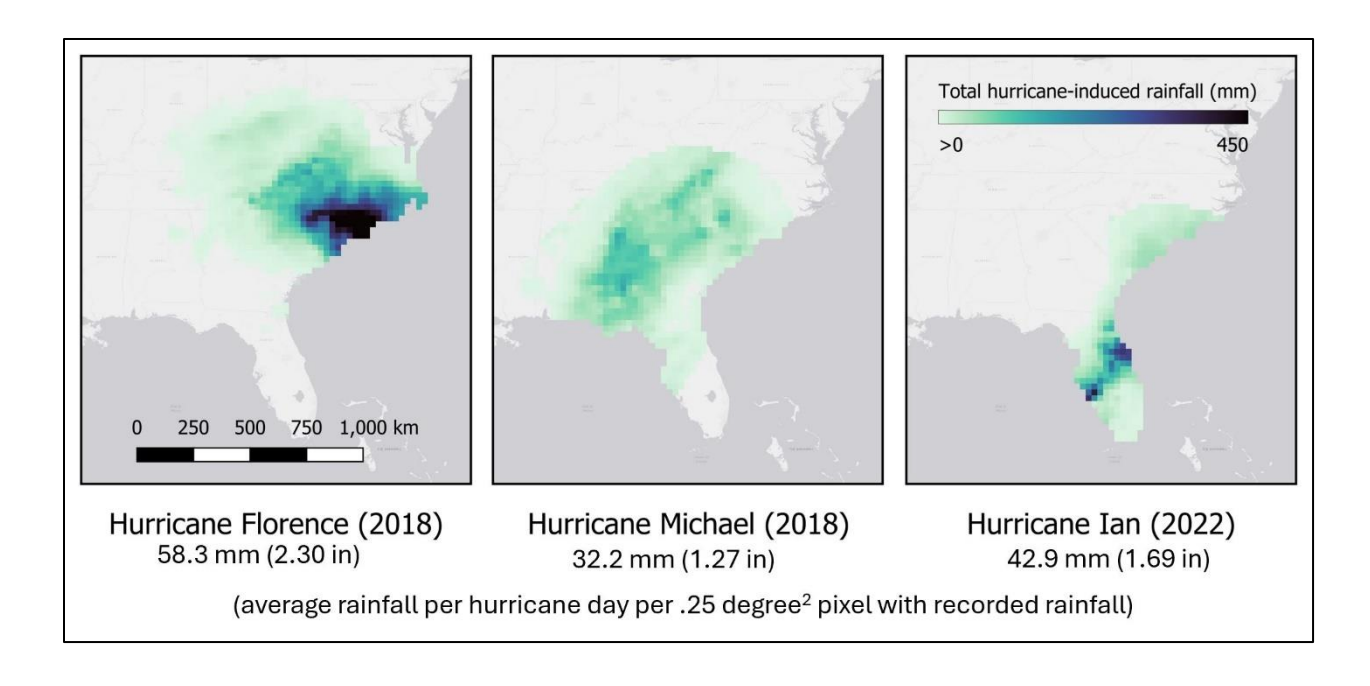


Figure 11: Total average hurricane-induced rainfall for hurricanes Florence, Michael, and

Ian within space/time scope of study per .25 degree² pixel.

The results in Figure 11 align with information gathered through background research on the three hurricanes. For Florence, which has the maximum average rainfall at 58.3 mm, rainfall was the main hazard and cause of many deaths. For Michael, rainfall was not the main hazard, and the system was only responsible for flash flood-related deaths after extratropical transition, which is not examined in this study. Michael had an average rainfall of 32.2 mm. Ian was somewhere in the middle, with rainfall leading to impacts in a smaller area. Accordingly, the average rainfall at 42.9 mm was in between that of Florence and Michael.

Statistic	Florence	Michael	Ian
Pixels w/ rainfall	1170	1061	364
Min (mm)	0.021	0.039	0.026
Max (mm)	602.425	151.305	383.950
Range (mm)	602.404	151.266	383.924
Sum (mm)	68227.279	34194.722	15629.891
Mean (mm/pixel)	58.314	32.229	42.939
std_dev	104.354	31.059	64.753
sum_of_squares	12730234.819	1022557.217	1522035.404

Table 9: Basic statistics for total rainfall data for each storm, based on the data displayed in Figure 11.

Table 9 shows the basic statistics for the totals shown in Figure 11. Note that Michael's is the same as Table 6 due to the storm lasting for only one day. For Florence and Ian, these statistics represent the data for the average daily rainfall of every pixel containing rain during the duration of each hurricane.

To determine which significance test to use for analyzing rainfall differences, a Shapiro-Wilk Normality test was performed in R to assess the normality of each set of rainfall measurements. Results are shown in Table 10. For all three hurricanes, the p-value was less than 0.05, indicating that the null hypothesis (H_0) should be rejected and the alternative hypothesis (H_1) should be assumed. Therefore, it can be assumed that the sample does not come from a normal distribution.

H₀: The sample comes from a normal distribution.

H₁: The sample does not come from a normal distribution.

Hurricane	W	p-value
Florence	0.60156	< 2.2e-16
Michael	0.87918	< 2.2e-16
Ian	0.62283	< 2.2e-16

Table 10: Results of Shapiro-Wilk Normality Test

Because the data sets do not follow a normal distribution, validating statistical significance required the use of a test that does not assume normality. For this purpose, the Mann-Whiteny U test was deemed most appropriate. This test compares two data sets at a time, so results are described for all possible pairings (Florence and Michael, Florence and Ian, and Michael and Ian). Results are shown in Table 11. The null and alternative hypotheses are described below.

H₀: The hurricane pairs have the same distribution of total rainfall.

H₁: The hurricane pairs do not have the same distribution of total rainfall.

Hurricane Pairs	W	p-value
Florence and Michael	673377	0.0005251
Florence and Ian	237816	0.0007509
Michael and Ian	195014	0.7778

Table 11: Results of Mann-Whitney U Test

These results show the significance of the differences between total average rainfall per pixel for each hurricane. Florence and Michael and Florence and Ian were found to be strongly significantly distinct. The p-values for these comparisons were both well less than .001, indicating that H₁ can be accepted at the 99.9th percentile. However, for Michael and Ian, there was not a significant difference that could be indicated by the Mann-Whitney U test. With the result of 0.778, the null hypothesis could not be rejected, and we are unable to assume that the distributions of rainfall for Michael and Ian are different.

4.2 Comparing EROs to flash flooding observations

Using QGIS, maps were produced that compare Day 3, 2, 1 and one ERO forecasts to the observed extent of flash flooding based on a Stage IV rainfall flash flood proxy. Figures 12-15 show these evolutions for each day of the storm being analyzed. From a visual analysis, the maps for Florence seem to display a generally accurate depiction of where flash flooding was to take place. For all days, the High category seems to clearly align better with the actual extent of flash flooding as the date of the event gets closer.

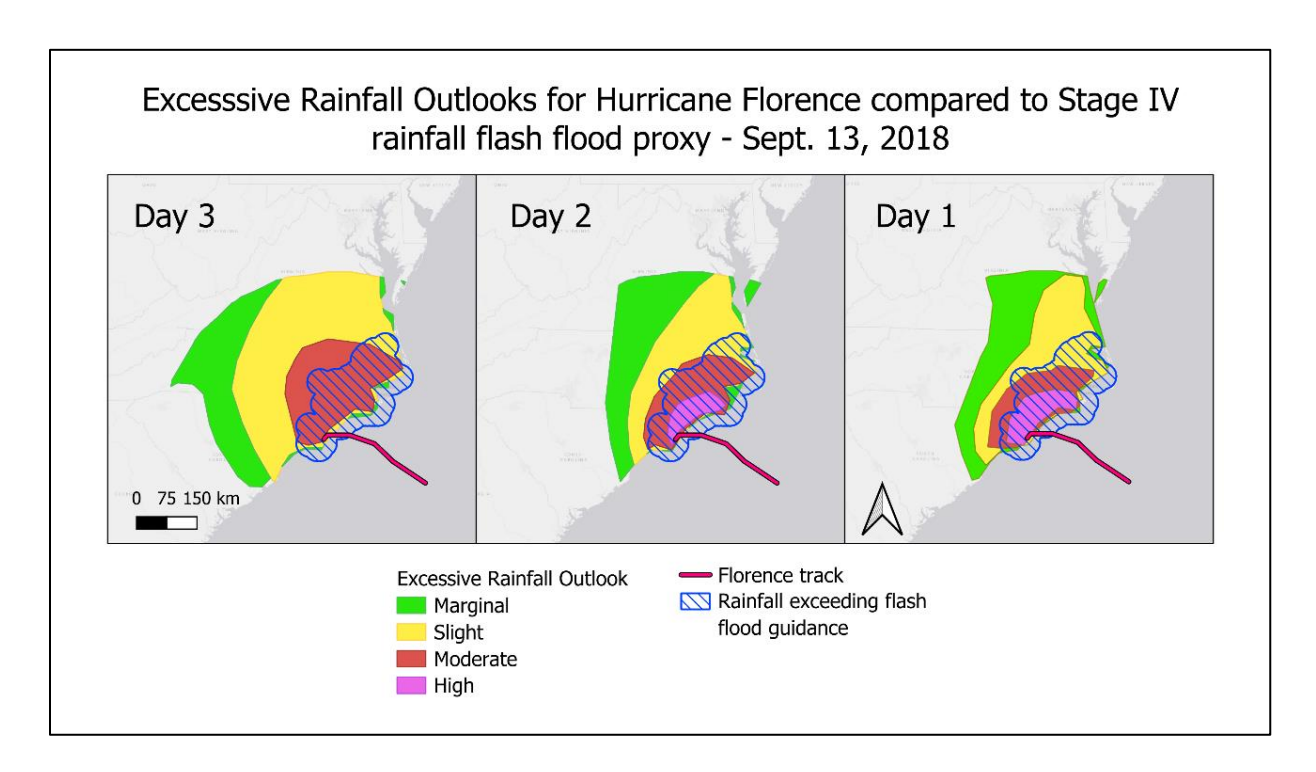


Figure 12: Excessive Rainfall Outlooks for Hurricane Florence compared to Stage IV rainfall flash flood proxy – 9/13/18

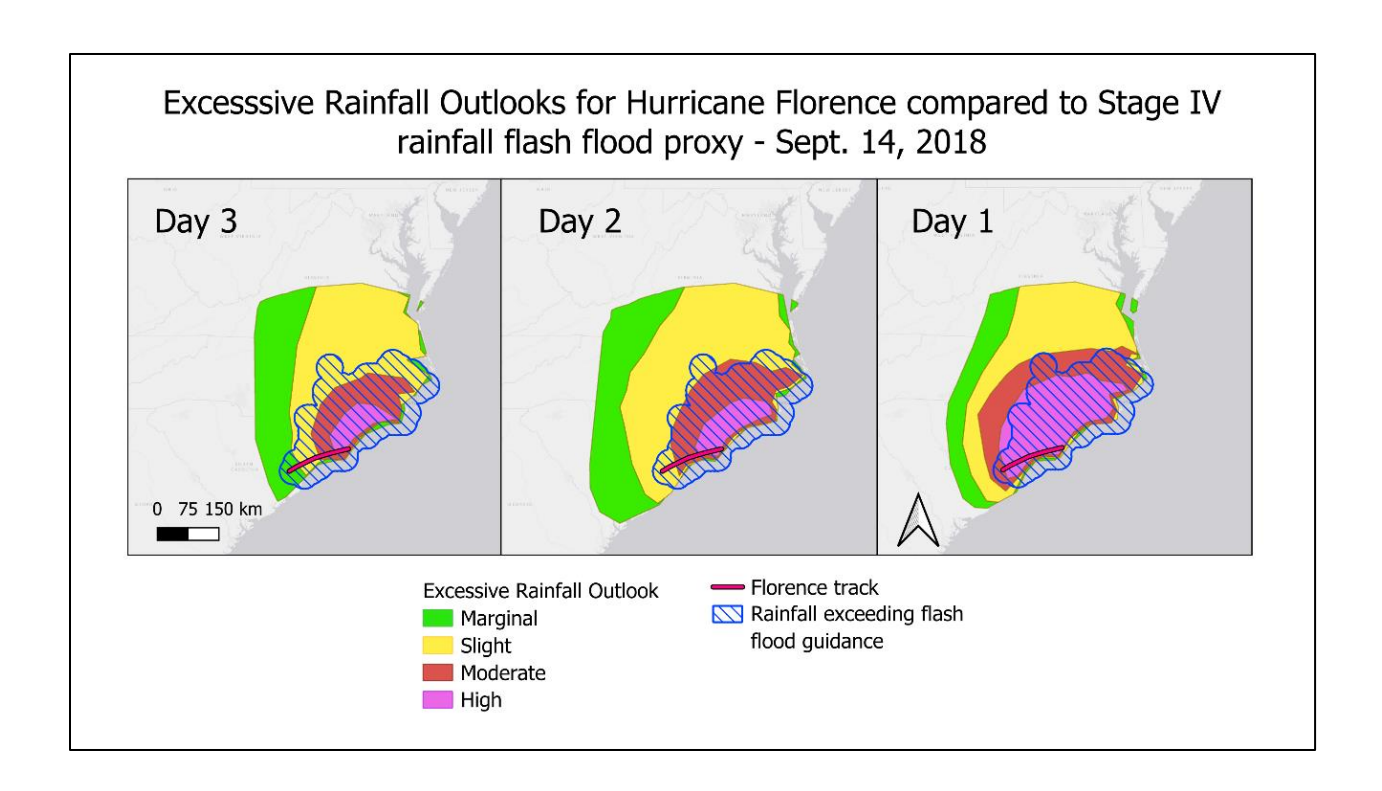


Figure 13: Excessive Rainfall Outlooks for Hurricane Florence compared to Stage IV rainfall flash flood proxy – 9/14/18

It should be noted that many of the EROs issued went out of the 500 km ROI at their periphery, so there could be some hurricane-related issuances that were not accounted for. For consistency, all EROs were clipped to the ROI. However, no flash flooding occurred outside of the ROI, according to the data from the proxy. Furthermore, most flash flooding was confined within the ERO contours for all days.

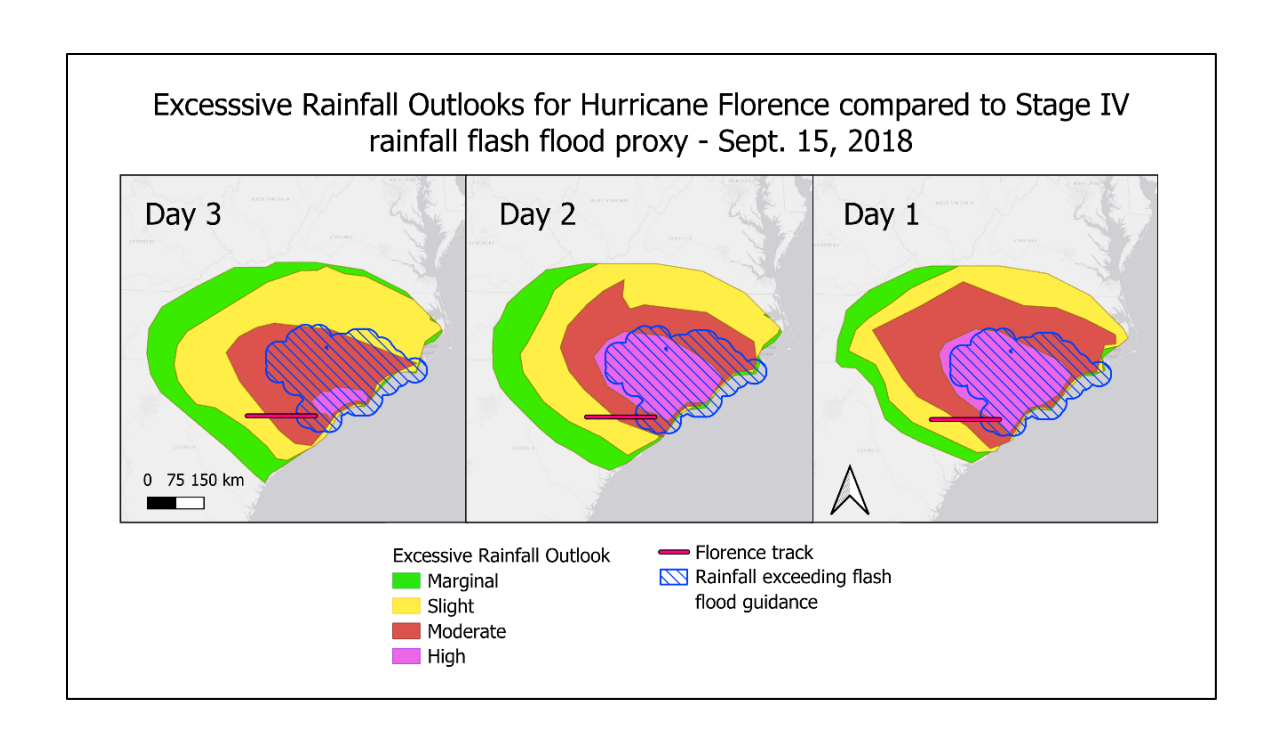


Figure 14: Excessive Rainfall Outlooks for Hurricane Florence compared to Stage IV rainfall flash flood proxy – 9/15/18

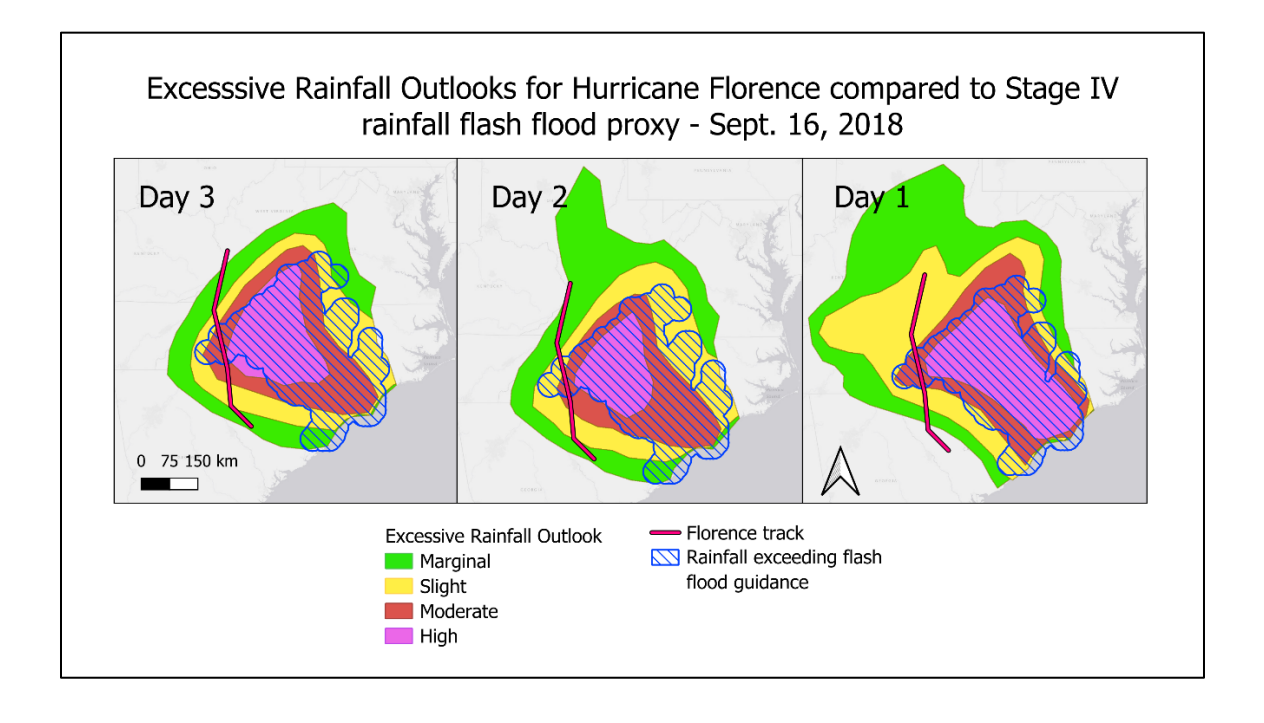


Figure 15: Excessive Rainfall Outlooks for Hurricane Florence compared to Stage IV rainfall flash flood proxy – 9/16/18

From a visual analysis, it seems that some Marginal and Slight outlook areas were overwarned across the maps. For example, in Figure 14, these contours contain minimal to no amount of the proxy. This is problematic as it could indicate overwarning, which could potentially contribute to warning fatigue among populations of affected areas if it occurs too often, resulting in people taking warnings less seriously. On the other hand, Figure 12 shows a potential example of underwarning for the Moderate category. Underwarning could lead to grave consequences, and this should also be analyzed further. A quantitative look at these disparities is performed in Section 4.2 and visualized in Table 12.

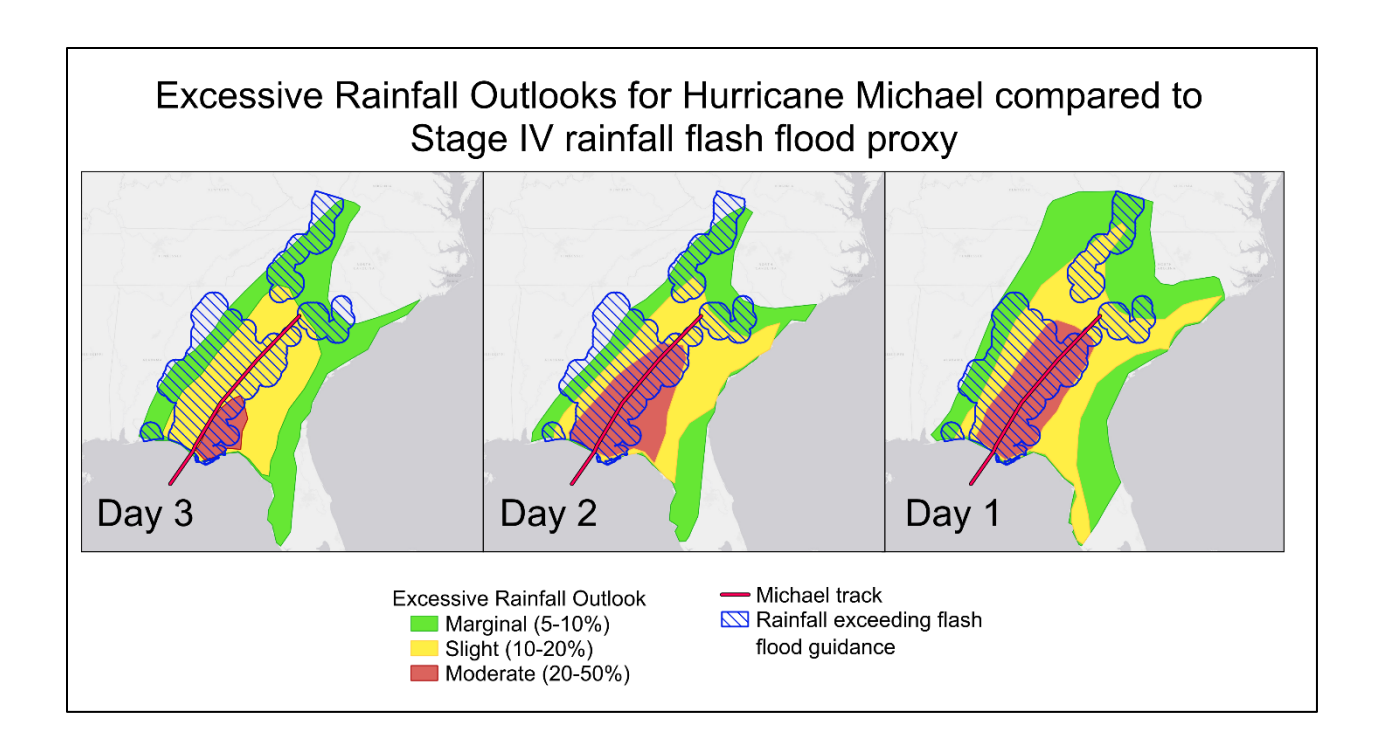


Figure 16: Excessive Rainfall Outlooks for Hurricane Michael compared to Stage IV rainfall flash flood proxy – 10/10/18

For Hurricane Michael, flash flooding tended to occur to the left of the storm track.

Notably, there were no High warnings issued during the day of study for this hurricane. This

indicates underwarning being a significant issue for the EROs issued during Michael. However, it should be noted that the forecast does appear to align more with the observation as the day of the event is approached. This suggests forecasts getting better over time, though in an ideal world, forecasts would be as accurate as possible as early as possible. A visual analysis suggests that underwarning was present for all three categories, which is exacerbated by the lack of any High contours. Again, this is discussed quantitatively in Section 4.2.

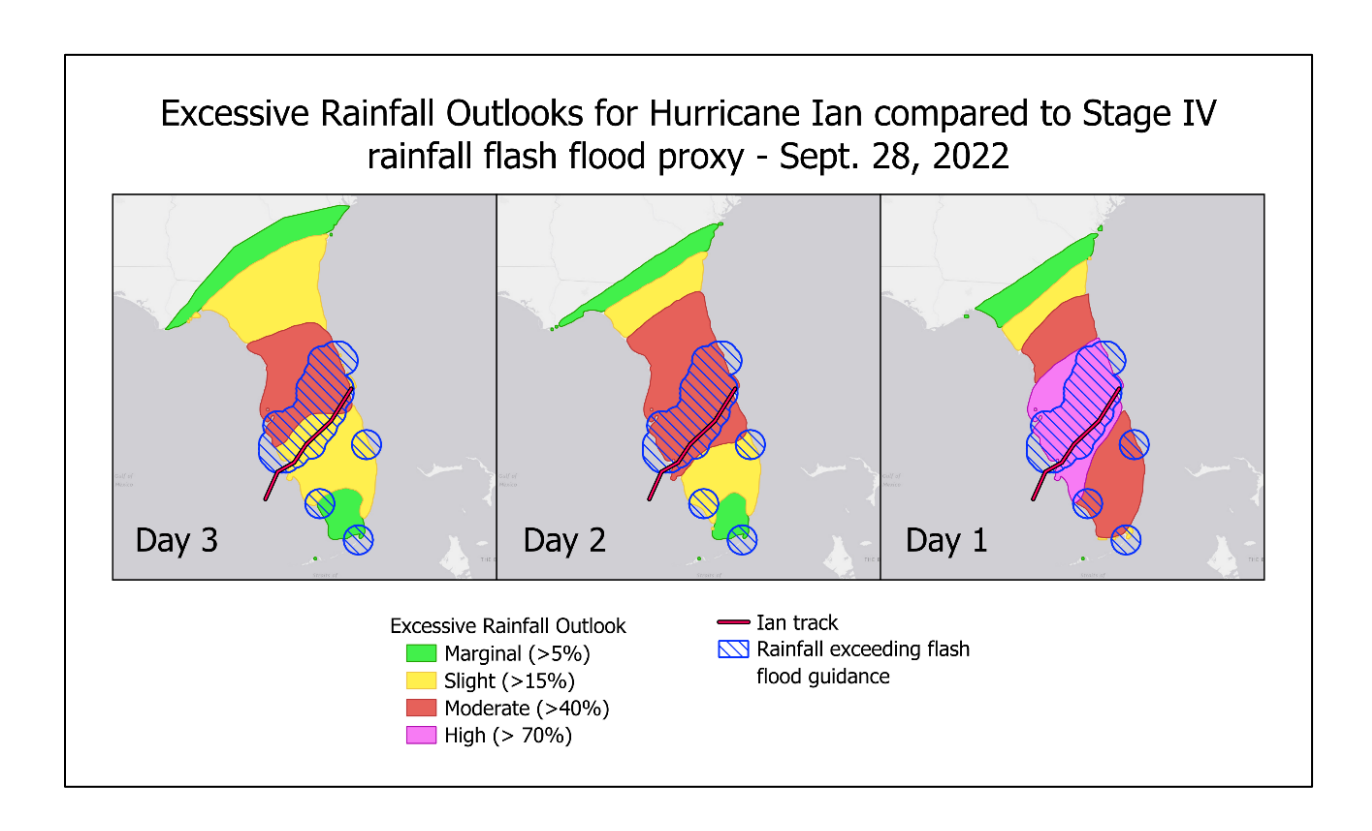


Figure 17: Excessive Rainfall Outlooks for Hurricane Ian compared to Stage IV rainfall flash flood proxy – 9/28/22

Like with Michael, flash flooding for Ian tended to the left side of the storm track for both 9/28/22 and 9/29/22. Based on background research, there were a lot of difficulties with forecasting the track of Ian and this seems to be shown in the EROs as well. Ian was predicted to

go through the Tampa area up until very close to landfall, when the track shifted to predict landfall around Fort Myers. It seems this track error is a factor in both Day 3 and Day 2 shown in Figures 17 and 18. We can also see the dramatic changes in contours in Figure 18 that indicate this uncertainty. By Day 1, the contours appear more accurate, but the High area is not well-aligned with the observed flash flooding.

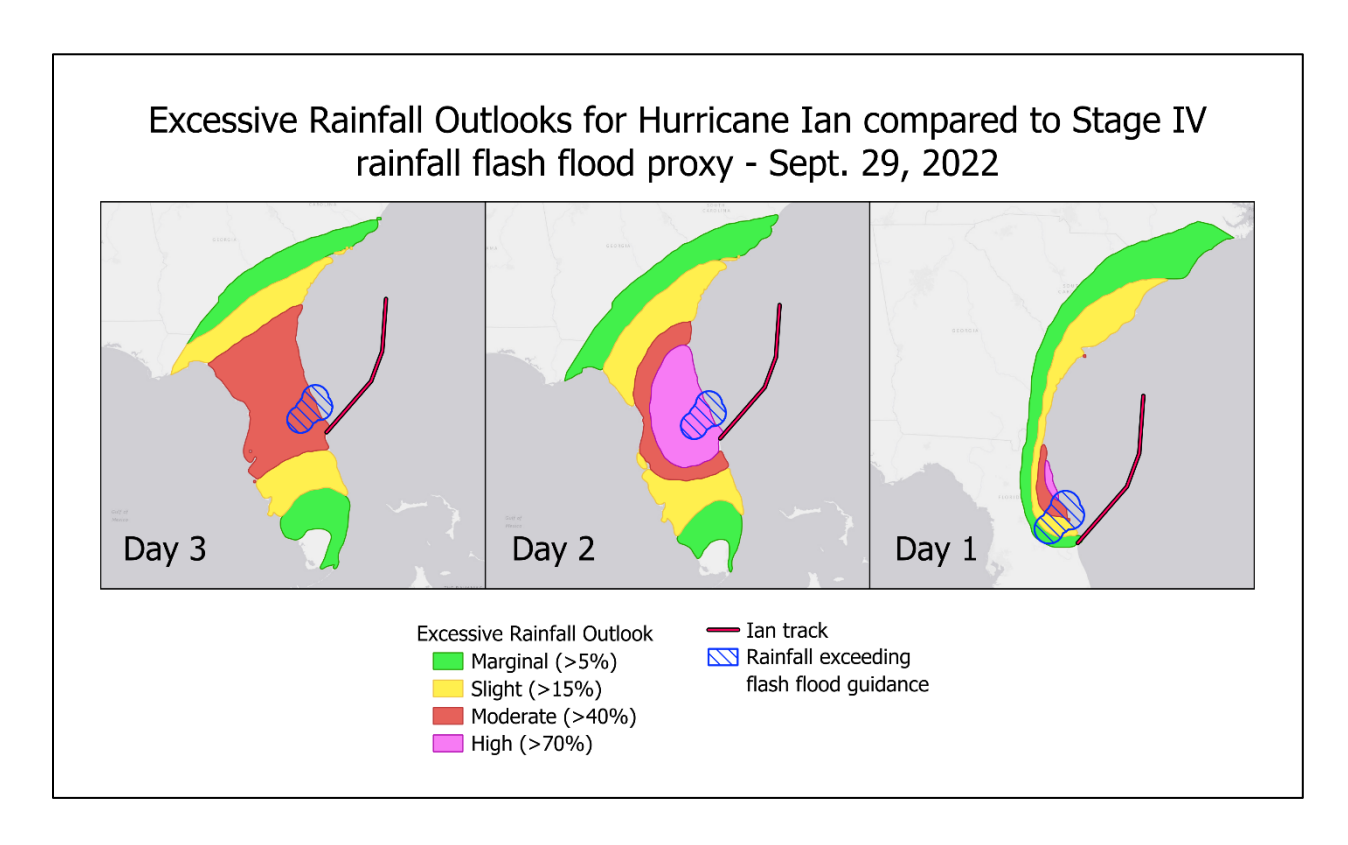


Figure 18: Excessive Rainfall Outlooks for Hurricane Ian compared to Stage IV rainfall flash flood proxy – 9/29/22

For 9/28/22, the Day 3 and 2 forecasts omitted a High outlook, representing potential underwarning. By Day 1, however, much of the area was overwarned for Marginal, Slight, and Moderate categories. Overwarning was also prominent on 9/29/22 for all forecast days, though Day 1 seems to suffer most from contours that were slightly too northward. If not for this, it

appears that the forecast would be reasonably representative of the actual extent of flash flooding.

The quantitative part of this verification consists of comparing observed fractional coverage to expected fractional coverage. Fractional coverage is defined as the area of overlap of flash flooding and a contour divided by the total area of the contour. This is then compared to the expected fractional coverage, which is based on the criteria for each ERO category. As discussed in the background, the ERO categories (Marginal, Slight, Moderate, High) were defined differently before 2022 (5-10%, 10-20%, 20-50%, 50-100%, respectively) and after early 2022 (>5%, >15%, >40%, >70%). Because Florence and Michael occurred in 2018 while Ian occurred in late 2022, all fractional coverage was compared to both the old definitions and new definitions in order to assess the redefinition of the metric.

Hurricane	Date	Forecast Day	overlap	Marginal obsexp. (old)			Slight obsexp. (old)	Slight obsexp. (new)	Moderate overlap (%)		Moderate obsexp.	High overlap (%)	High obsexp. (old)	High obsexp. (new)
			` ′	` ′	(` ′	` ′	(` ′	` ′	(/	` ′	` ′	` ′
Florence	9/13/2018	3	2.17	-2.83	-2.83	6.76		-8.24						
		2	3.25	-1.75	-1.75	15.7			86					_
		1	3.08	-1.92	-1.92	25.7		0	72.5					-
	9/14/2018	3	11	1	0	30.7		0	100					_
		2	1.56	-3.44	-3.44	14.1								_
		1	4.02	-0.98	-0.98	3.33		-11.67			-	93.7		
	9/15/2018	3	0.97	-4.03	-4.03	5.29	-4.71	-9.71	63.3	13.3				
		2	2.57	-2.43	-2.43	0.91	-9.09	-14.09	27.2				_	
		1	1.68	-3.32	-3.32	1.82	-8.18	-13.18	15.4	-4.6	-24.6	88	0	0
	9/16/2018	3	10.2	0.2	0	42.4	22.4	2.4	73.8	23.8	3.8	92.9	0	0
		2	5.63	0	0	44.4	24.4	4.4	82.1	32.1	12.1	99.1	0	0
		1	1.5	-3.5	-3.5	14.5	0	-0.5	71.2	21.2	1.2	99.5	0	0
Michael	10/10/2018	3	39.2	29.2	24.2	54.3	34.3	14.3	78.9	28.9	8.9	n/a	n/a	n/a
		2	40.1	30.1	25.1	33.1	13.1	0	76.4	26.4	6.4	n/a	n/a	n/a
		1	21.2	11.2	6.2	38.5	18.5	0	86.7	36.7	16.7	n/a	n/a	n/a
Ian	9/28/2022	3	8.32	0	0	19.6	0	0	50.1	0.1	0	n/a	n/a	n/a
		2	4.78	-0.22	0.22	12.8	0	2.2	48.3	0	0	n/a	n/a	n/a
		1	0	-5	5	3.47	-6.53	11.53	11.7	-8.3	28.3	68.3	0	-1.7
	9/29/2022	3	0	-5	5	0	-10	15	8.52	-11.48	31.48	n/a	n/a	n/a
		2	0	-5	5	0	-10	15	0	-20	40	15.3	-34.7	54.7
		1	3.33	-1.67	1.67	10.1	0			0	7.5			

Table 12: Fractional coverage and deviation from expected values for each category of each forecast for each day of each hurricane, for old and new ERO definitions

In Table 12, the results of the process described above is shown. Figure 19 depicts these differences as charts to get a better visual sense of the difference between expected and observed fractional coverages. Positive values represent underwarning, while negative values represent overwarning. The closer the values are to 0, the more accurate the forecast was.

Looking at the table and charts, we can generally see that for Florence and Michael, the new ERO definitions produce more accurate (closer to 0) results. With Ian, the results for the new definitions tended to deviate more from 0. It is also interesting to analyze how the EROs evolve over time for each day of the storm. In some cases, like for Florence under the old ERO definition for 9/14 and 9/15, the values tend closer to 0 as we get closer to the day the forecast is issued for. In other cases, the values seem to get less accurate, like with Ian. This could be due to the fact that no High warnings were issued for Ian until the final day, as well as the inaccurate track forecasting as discussed earlier.

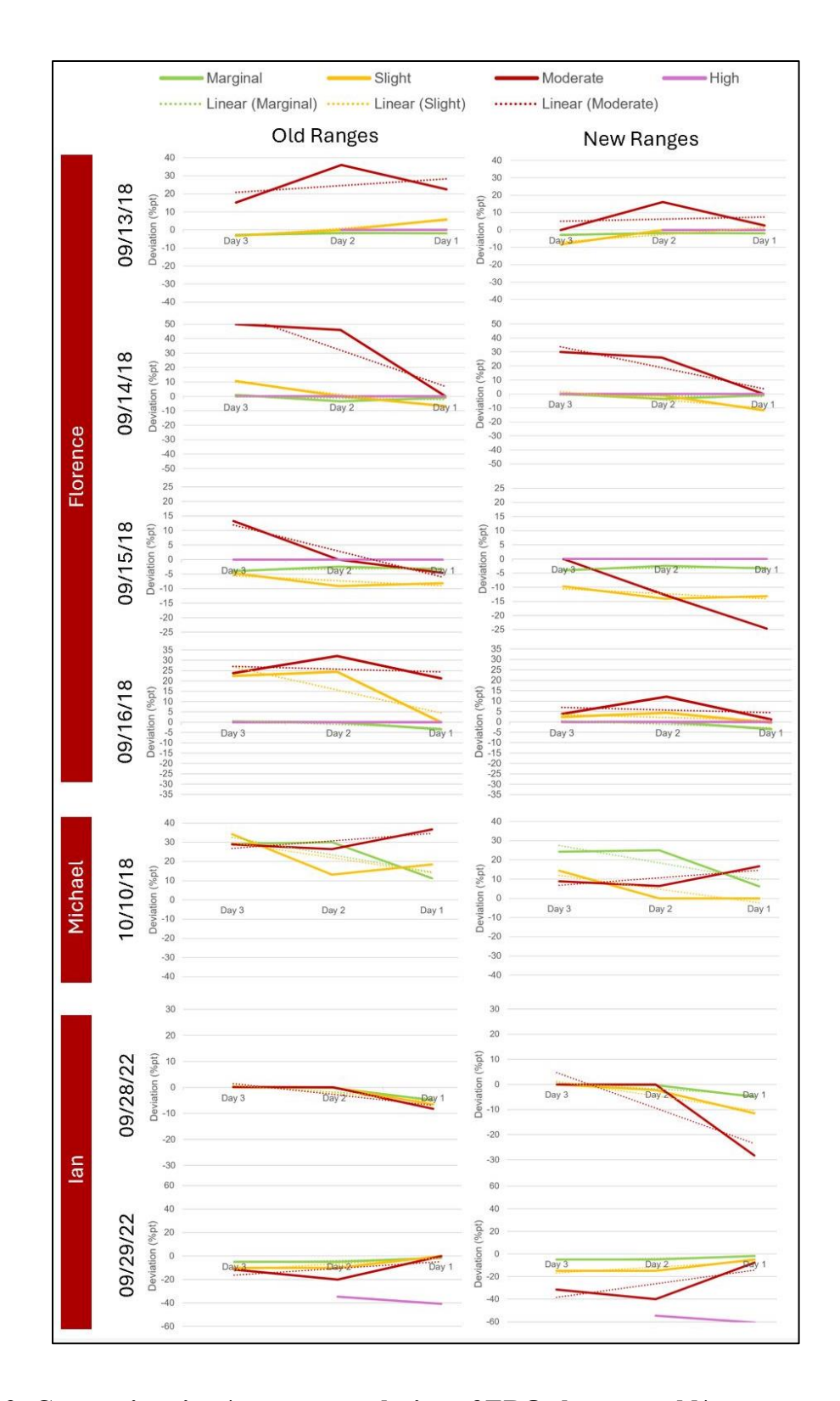


Figure 19: Comparing time/accuracy evolution of EROs between old/new ranges (positive values=underestimation, negative=overestimation) (note that ranges differ per hurricane)

To verify the ERO forecasts against observations by obtaining a quantitative score of ERO performance, Fractional Brier Scores and Fractional Skill Scores were calculated. The Fractional Brier Score (FBS) is analogous to the typical Brier Score used for forecast verification, but works by comparing forecasted fractional coverage to observed fractional coverage rather than comparing fractional forecasts to binary outcomes. Like with the Brier Score, the FBS deems a forecast more accurate the closer to 0 it is. However, it is inappropriate to compare FBSs to one another, as the definition changes for every calculation. The Fractional Skill Score (FSS) combats this. The FSS takes the worst possible FBS (WFBS) for the particular calculation and compares it to the calculated FBS. The equations used are shown below. The resulting FSS is more accurate the closer to 1 it is.

FBS =
$$\frac{1}{I} \sum_{i=1}^{I} (NP_{i,f} - NP_{i,o})^2$$

WFBS =
$$\frac{1}{I} \left(\sum_{i=1}^{I} NP_{i,f}^{2} + \sum_{i=1}^{I} NP_{i,o}^{2} \right)$$

$$FSS = 1 - \frac{FBS}{WFBS}.$$

Results for each hurricane for both new and old ERO definitions are shown in Table 13. The FBS scores all appear fairly close to 0, but as discussed above, this tells us little about how they compare to each other. Accordingly, the WFBS scores were calculated, allowing for FSS scores to be determined. All scores were greater than 50%, indicating that the EROs were useful according to the standards described in Necker et al. 2024, and all were additionally greater than 75%, representing significantly higher skillfulness than the 50% standard. Additionally, all FSS scores for the new ERO definition were higher than those for the old ERO definition, validating

the 2022 choice to change the definition. Hurricane Florence had the most accurate EROs across both categories, while Hurricane Ian had the least accurate EROs. This aligns well with the visual analysis of the EROs vs observed flash flooding for each hurricane discussed previously in this section, shown in figures 12-18.

Hurricane	FBS_old	FBS_new	WFBS_old	WFBS_new	FSS_old	FSS_new
Florence	0.0222	0.0098	0.2669	0.3391	0.9168	0.9710
Michael	0.0717	0.0206	0.4189	0.5361	0.8288	0.9615
Ian	0.0180	0.0230	0.0839	0.1101	0.7855	0.7912

Table 13: FBS, WFBS, and FSS results for each hurricane under old and new ERO definitions.

4.3. Rainfall, Social Vulnerability, and Disaster Declaration in Florence

Figure 20 shows the official FEMA-approved disaster declaration designations in North Carolina after the Hurricane Florence event in September 2018. As discussed in Section 2.4, these designations can include individual assistance and/or public assistance, with categories A-G representing full-spectrum public assistance. This figure can be compared with Figure 21, which shows Hurricane Florence's rainfall and 2018 demographic statistics for North Carolina counties.

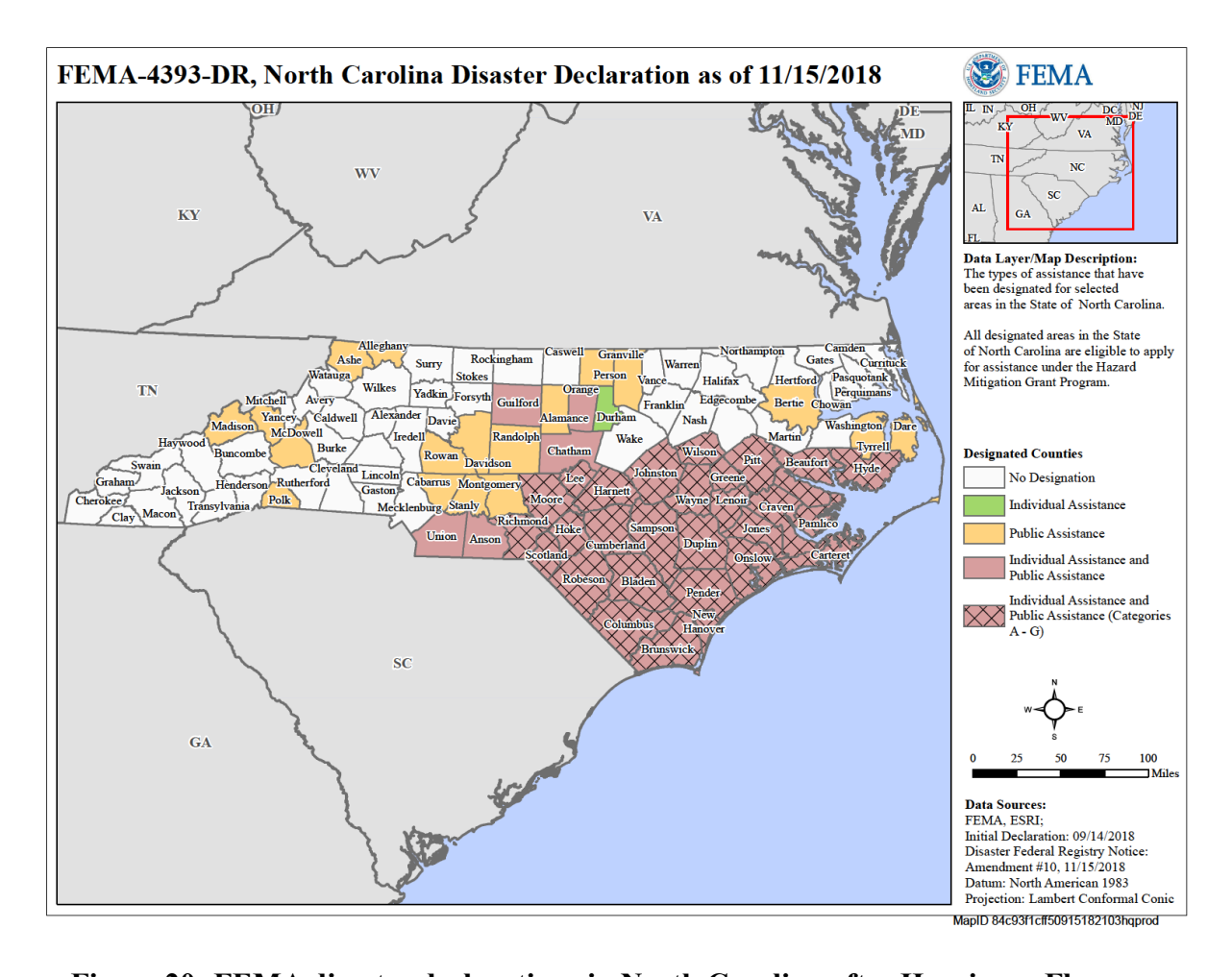


Figure 20: FEMA disaster declarations in North Carolina after Hurricane Florence.

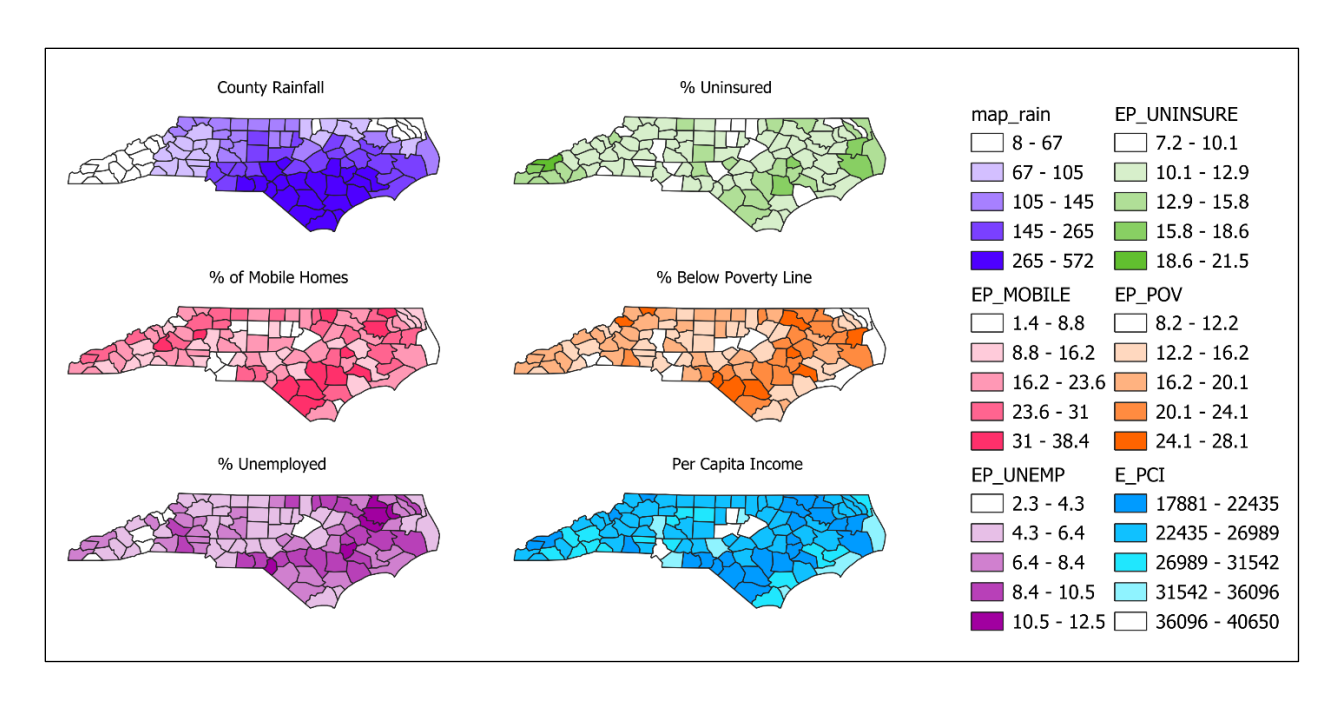


Figure 21: Florence total rainfall and social vulnerability factors by county. Rainfall from CPC-Unified dataset, social data from SVI (2018).

This visual analysis is important as it provides insights into why a particular county may have been designated the way it was. For example, Wake County, depicted in Figure 20, experienced a significant amount of rainfall according to Figure 21 but was not assigned any federal disaster relief. Looking at the demographic factors in Figure 21, it can be seen that Wake County is consistently resilient by all the listed factors, as it is high in Per Capita Income and low in all hardship measures. This provides preliminary evidence that social factors were taken into account when providing deferral relief after Hurricane Florence, however, certain distinctions are less clear. Randolph County only received public assistance, not individual, despite being similarly or more vulnerable than nearby Guilford County, which received both after a similar amount of rainfall.

To perform the multinomial logistic regression model aspect of this analysis, first, a rainonly model was made for Florence's impact in North Carolina. After training the model in R, a
process that calculated the optimal coefficients for each variable, the model had a 73% accuracy
rate when predicting disaster designation based on county rainfall alone. To examine these
results further, we can look at the coefficients (Table 14) and corresponding p-values (Table 15).
A closer look at predicted designations versus true designations is available in Table 18. The
possible designations are shown in Figure 20, and the shorthand key for each value in the table is
listed below.

- 0 No designation
- 1 Individual Assistance
- 2 Individual Assistance and Public Assistance
- 3 Individual Assistance and Public Assistance (Categories A-G)

4 - Public Assistance

In Tables 14 and 15, each row compares the odds of the 0 (no designation) category to category 1, 2, 3, or 4. The coefficient is only notable if the corresponding p-value indicates that the coefficient is significant. For the rain-only model, the coefficients are significant for all categories except 1, which is likely due to there being only one data point assigned to the Individual Assistance Only category (see Figure 20). Positive coefficients indicate that as rainfall increases, the likelihood of the county being assigned the designation vs no designation increases. With this baseline accuracy, we can go on to produce a model that takes SVI variables into account.

	(Intercept)	Coefficients: rain\$Band1
1	-7.685600	0.03364345
2	-10.777711	0.05997723
3	-11.865540	0.07027526
4	-2.880751	0.01917204

Table 14: Coefficients for Rain-Only Model (green shading = significant to p < .05)

	(Intercept)	P Values: rain\$Band1
1	3.099274e-02	1.583157e-01
2	6.840698e-05	2.056865e-04
3	1.223372e-05	1.463243e-05
4	3.442519e-04	6.310509e-03

Table 15: p-values for Rain-Only Model (green shading = significant to p < .05)

Tables 16 and 17 show the coefficients and p-values for this more complex rain + SVI model. After going through the same process of optimizing coefficients and assessing ultimate accuracy, this model has a 79% accuracy of predicting the correct category, which is notably greater than the rain-only model. Again, the significant p-values and their corresponding coefficients are highlighted.

	(Intercep	rain\$Ban	EP_UNIN	EP_UNE	EP_POV	EP_MOB	E_PCI
	t)	d1	SUR	MP		ILE	
1	-5.8426	-0.5385	5.6257	-10.118	3.3598	-10.557	1.3383e-03
2	-17.375	0.0603	-0.1909	-0.0412	0.1252	0.0053	2.2418e-04
3	-20.442	0.0674	0.4108	0.1886	0.0499	0.0074	6.8628e-05
4	3.4398	0.0211	-0.0931	-0.2182	-0.0530	0.0173	-1.3691e-04

Table 16: Coefficients for Rain + SVI Model

	(Intercep t)	rain\$Band1	EP_UNINS UR	EP_UNEM P	EP_POV	EP_MO BILE	E_PCI
1	-5.8426	0.0000e+0	0.0000e+0	0.0000e+0	0.0000	0.0000	0.9045
2	-17.375	7.1623e-7	0.0000e+0	5.2637e-5	0.0002	0.9139	0.0014
3	-20.442	6.8854e-7	0.0000e+0	0.0000e+0	0.4100	0.8356	0.3650
4	3.4398	3.7471e-3	1.2001e-10	0.0000e+0	0.3568	0.6800	0.0008

Table 17: p-values for Rain + SVI Model

In this model, we can see which SVI variables are most significant when predicting county disaster designation. Rainfall, percent uninsured, and percent unemployed all had universally significant impacts on the accuracy of the model. On the other hand, percent below the poverty line, percent of mobile homes, and per capita income had variable outcomes, with improved accuracy for some categories but not for others.

For further insight into the testing outcomes of the model, Table 18 shows the predicted designations for 25 counties versus their actual designations. Predictions for both models (rain and rain + SVI) are shown, with highlighted numbers representing a correct prediction. From this closer analysis, we can note particular counties, such as Ashe and Chatham, where SVI variables contributed to a correct prediction. In Ashe County, the consideration of rain only resulted in an incorrect prediction of no federal assistance. However, when SVI variables were considered, the model gave a correct prediction of public assistance. On the other hand, for Chatham County, the rain only model predicted more assistance (Individual & Public A-G) than was needed. When considering the low social vulnerability of the county, the model correctly went on to predict that less assistance was needed.

County	Designation	Rain Only prediction	Rain + SVI prediction
Alamance	4	0	0
Alexander	0	0	0
Alleghany	4	0	0
Anson	2	3	3
<u>Ashe</u>	4	0	4
Avery	0	0	0
Beaufort	3	3	3
Bertie	4	0	0
Bladen	3	3	3
Brunswick	3	3	3
Buncombe	0	0	0
Burke	0	0	0
Cabarrus	4	4	4
Caldwell	0	0	0
Camden	0	0	0
Carteret	3	3	3
Caswell	0	0	0
Catawba	0	0	0
Chatham	2	3	2
Cherokee	0	0	0
Chowan	0	0	0
Clay	0	0	0
Cleveland	0	0	0
Columbus	3	3	3
Craven	3	3	3

Table 18: Designations vs. predicted designations for 25/100 counties.

These results should be considered in the context of the small sample size, which included only the 100 counties of North Carolina, and the fact that these models were only tested on one hurricane event with extreme rainfall. Adding other hazard measures to the model, such as max wind speed or tornado presence, could result in increased accuracy of predictions.

Though there was a clear increase from the accuracy of the rainfall-only model (73%) to the

accuracy of the rainfall plus SVI model (79%), it is difficult to say how significant this difference is. It is also uncertain whether the SVI variables contributed to directly the designations or whether the relationship was indirect or by chance.

CHAPTER 5

CONCLUSION

5.1. Discussion

The results of this thesis reveal various components of how hurricane rainfall hazard is characterized. Because of the nature of this study, which only looks at three hurricanes, it is difficult to draw conclusions beyond the hurricanes considered in this analysis. However, the methodology can provide a framework for future studies that consider a larger sample of hurricane rainfall data, which would be particularly useful for the ERO verification conducted as part of Research Question 2.

For the first research question concerning how rainfall was distributed over space and time for Hurricanes Florence, Michael, and Ian, it can be concluded from a visual analysis and by comparing basic statistics that all three had different rainfall profiles in a qualitative sense. However, when testing for quantitative significant differences in the distributions, it was found that, by the chosen method, Michael and Ian were not significantly different from each other. From this result, we can conclude that even for seemingly very different hurricane profiles, rainfall is not necessarily significantly diverse.

The second aspect of this thesis concerned comparing EROs with the actual extent of flash flooding during each hurricane. The strongest conclusions can be drawn when looking at the Fractional Skill Scores for each definition. Florence had the most accurate EROs, Michael

had the second most accurate EROs, and Ian had the least accurate EROs. This indicates that ERO accuracy differs by each hurricane and may be highly dependent on track predictions and other factors that are not necessarily at play in EROs for non-hurricane events. Additionally, there was not a consistent increase in accuracy from Day 3 to Day 1 measurements. This is problematic, as forecasts should theoretically consistently get better the closer we get to the anticipated event. We can also conclude that the new ERO definition is more accurate than the old ERO definition, though, again, the small sample size does not allow us to test for the significance of these differences.

Finally, with Research Question 3, it can be concluded that rainfall likely played a factor in county-level FEMA disaster declaration designations, and that social vulnerability variables potentially played a role. It should be noted that the accuracy did not decrease with the SVI variables, so we can likely rule out there being a negative relationship. Again, a larger sample size is required to draw further conclusions about how these SVI variables played a role compared to the role of rainfall. Furthermore, there are many variables unaccounted for that may have confounded the results.

These conclusions can be applied in varied ways. The successful verification of the skillfulness of EROs supports their future use for warning populations of flash flooding during hurricanes. Emergency managers should take ERO issuances seriously as early as Day 3 in order to provide information to regions which may be at risk of experiencing flash flooding. In particular, any area designated with a High outlook should be warned as early as possible, as fractional coverage analysis showed that issuances of this category are highly accurate, even early on. Warnings based on EROs should include actionable information to prevent harm to life, infrastructure, and property. When determining the recommended action (i.e. shelter in place or

evacuate), local factors like elevation, water management infrastructure, and structural soundness should be considered. Accordingly, blanket statements of recommended actions at, say, the county level may not be appropriate. Individuals will need to play a role in their own decisions. In order for the public to make informed decisions, it must be ensured that EROs are well understood. Research on the social science side of risk communication should be performed, looking at how people perceive EROs and what preventative actions they end up taking based on the messaging. Other metrics, such as the Extreme Rain Multiplier discussed earlier, could be evaluated as well and compared to the conceivability of EROs.

5.2. Future Work

Future research should continue to validate the efficacy of EROs under hurricane conditions. These validations can become part of NHC Tropical Cyclone Reports for all US-landfalling tropical cyclones. The utility of verifying EROs in Tropical Cyclone Reports is already demonstrated by the newly released report for Hurricane Helene (Hagen et al. 2025). Though the report utilizes a different verification method (practically perfect rather than fractional coverage), it represents what is likely the first time that ERO verification has been included in a Tropical Cyclone Report. It is clear that the utility of verifying EROs in the context of hurricanes has been recognized, and future work should continue in this direction.

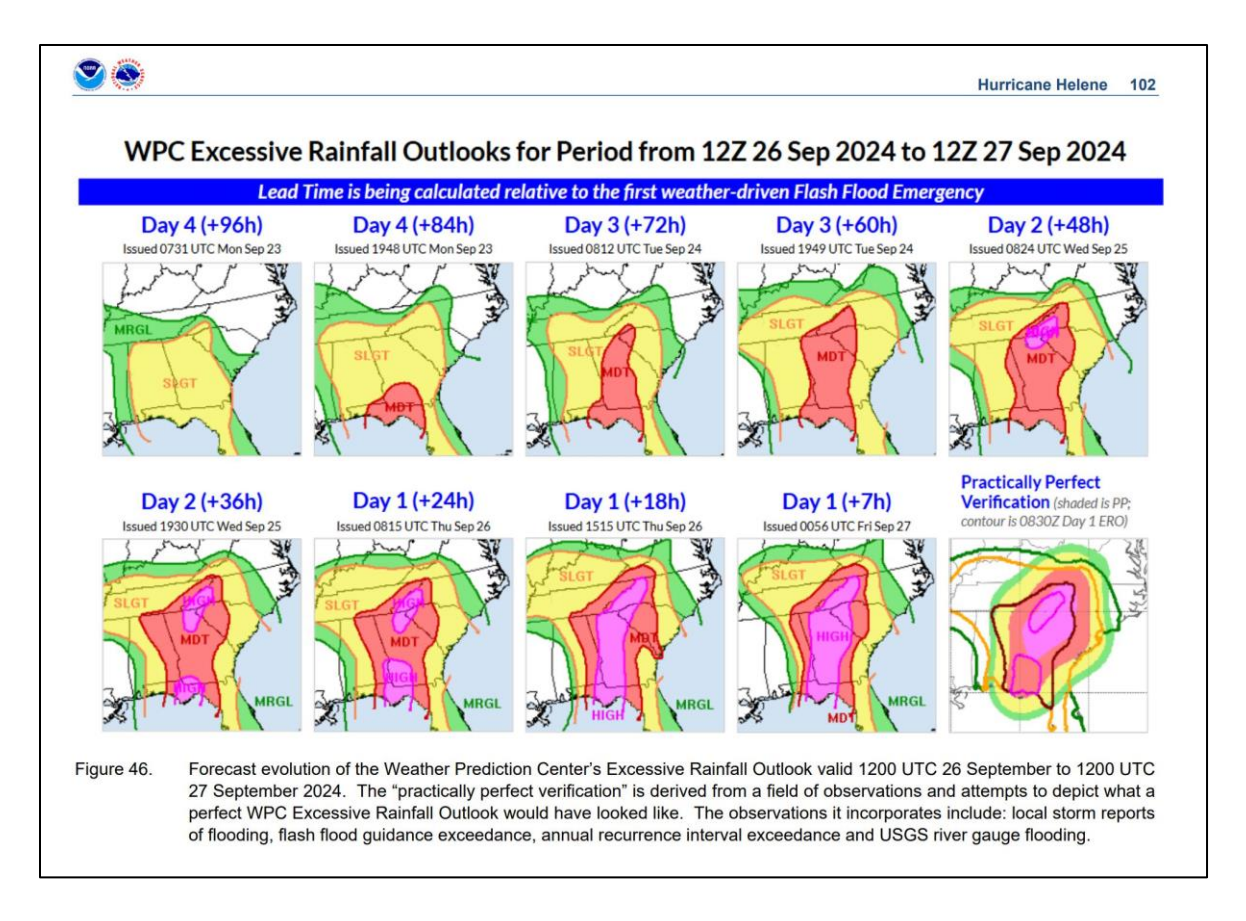


Figure 22: ERO forecast verification for Hurricane Helene (2024) as seen in the Tropical Cyclone Report by Hagen et al. 2025.

Expanding the space and time scope of this work is also an important measure to be taken. With this thesis project only covering a select number of recent hurricanes in the southeast, it would be interesting to see similar methods performed for hurricanes making landfall in other parts of the United States and at different points in history. A component of a temporal-based analysis could be determining how hurricane-induced rainfall has evolved as a result of climate change and investigating whether or not climate change has had an influence on the accuracy of forecasts. It will also be important for future work to continue to explore the role of rainfall and social variables in FEMA disaster declarations, especially considering the context mentioned in Section 2.4 that there can be political motivations behind approving disaster

declarations at the federal level. These political biases could be combatted by creating a more objective machine learning model based on a function of county-level hazards, exposure, and vulnerability to determine the most appropriate category of federal funding to distribute to each affected county. However, a model of this sort could obscure the nuance of disaster, and qualitative analysis of the situation should always be performed in tandem if such an algorithm were to be created. In all, it is clear that rainfall hazard should be considered in the context of exposure and vulnerability.

REFERENCES

Alipour, A., Yarveysi, F., Moftakhari, H., Song, J. Y., & Moradkhani, H. (2022). A Multivariate Scaling System Is Essential to Characterize the Tropical Cyclones' Risk. *Earth's Future*, *10*(5), e2021EF002635. https://doi.org/10.1029/2021EF002635

Bender, M. A., Knutson, T. R., Tuleya, R. E., Sirutis, J. J., Vecchi, G. A., Garner, S. T., & Held, I. M. (2010). Modeled Impact of Anthropogenic Warming on the Frequency of Intense Atlantic Hurricanes. *Science*, *327*(5964), 454–458. https://doi.org/10.1126/science.1180568

Beven II, J. L., Berg, R., & Hagen, A. (2019). *Hurricane Michael*. National Hurricane Center (NHC). https://www.nhc.noaa.gov/data/tcr/AL142018 Michael.pdf

Blake, E. S., & Zelinsky, D. A. (2018). *Hurricane Harvey*. National Hurricane Center (NHC). https://www.nhc.noaa.gov/data/tcr/AL092017_Harvey.pdf

Bosma, C. D., Wright, D. B., Nguyen, P., Kossin, J. P., Herndon, D. C., & Shepherd, J. M. (2020). An Intuitive Metric to Quantify and Communicate Tropical Cyclone Rainfall Hazard. Bulletin of the American Meteorological Society, 101(2), E206–E220.

https://doi.org/10.1175/BAMS-D-19-0075.1

Brennan, M., Brown, D., & Pope, L. (2023, August 8). *Recent Trends in Tropical Cyclone Fatalities in the United States*. The Front Page. https://blog.ametsoc.org/2023/08/08/recent-trends-in-tropical-cyclone-fatalities-in-the-united-states/

Bucci, L., Alaka, L., Hagen, A., & Beven, J. (2023). *Hurricane Ian*. National Hurricane Center (NHC). https://www.nhc.noaa.gov/data/tcr/AL092022 Ian.pdf

Camelo, J., & Mayo, T. (2021). The lasting impacts of the Saffir-Simpson Hurricane Wind Scale on storm surge risk communication: The need for multidisciplinary research in addressing a multidisciplinary challenge. *Weather and Climate Extremes*, *33*, 100335.

https://doi.org/10.1016/j.wace.2021.100335

Cao, Q., Knight, M., & Qi, Y. (2018). Dual-pol radar measurements of Hurricane Irma and comparison of radar QPE to rain gauge data. *2018 IEEE Radar Conference (RadarConf18)*, 0496–0501. https://doi.org/10.1109/RADAR.2018.8378609

Centers for Disease Control and Prevention/Agency for Toxic Substances and Disease Registry/Geospatial Research, Analysis, and Services Program. CDC/ATSDR Social Vulnerability Index 2020 Database US.

https://www.atsdr.cdc.gov/placeandhealth/svi/data documentation download.html

Centers for Disease Control and Prevention/Agency for Toxic Substances and Disease Registry/Geospatial Research, Analysis, and Services Program. CDC/ATSDR Social Vulnerability Index 2018 Database US.

https://www.atsdr.cdc.gov/placeandhealth/svi/data_documentation_download.html

Erickson, M. J., Albright, B., & Nelson, J. A. (2021). Verifying and Redefining the Weather Prediction Center's Excessive Rainfall Outlook Forecast Product. *Weather and Forecasting*, 36(1), 325–340. https://doi.org/10.1175/WAF-D-20-0020.1

Federal Emergency Management Agency (FEMA). (2024, July 22). How a Disaster Gets Declared | FEMA.gov. https://www.fema.gov/disaster/how-declared

Hagen, A.B., Cangialosi, J.P., Chenard, M., Alaka, L., & Delgado, S. (2025). *Hurricane Helene*. National Hurricane Center (NHC). https://www.nhc.noaa.gov/data/tcr/AL092024 Helene.pdf

Halverson, J., & Livingston, I. (2025). Hurricane Helene: Science and Impacts of a Superstorm. Weatherwise, 78(2), 16–25. https://doi.org/10.1080/00431672.2025.2457920

Husted, T., & Nickerson, D. (2014). Political Economy of Presidential Disaster Declarations and Federal Disaster Assistance. *Public Finance Review*, 42(1), 35–57.

https://doi.org/10.1177/1091142113496131

Intergovernmental Panel On Climate Change (IPCC). (2023). Climate Change 2021 – The Physical Science Basis: Working Group I Contribution to the Sixth Assessment Report of the Intergovernmental Panel on Climate Change (1st ed.). Cambridge University Press. https://doi.org/10.1017/9781009157896

KC, B., Shepherd, J. M., King, A. W., & Johnson Gaither, C. (2021). Multi-hazard climate risk projections for the United States. *Natural Hazards*, *105*(2), 1963–1976. https://doi.org/10.1007/s11069-020-04385-y

Knight, D. B., & Davis, R. E. (2007). Climatology of Tropical Cyclone Rainfall in the Southeastern United States. *Physical Geography*, 28(2), 126–147. https://doi.org/10.2747/0272-3646.28.2.126

Knight, D. B., & Davis, R. E. (2009). Contribution of tropical cyclones to extreme rainfall events in the southeastern United States. *Journal of Geophysical Research: Atmospheres*, *114*(D23). https://doi.org/10.1029/2009JD012511

Landsea, C. W., & Franklin, J. L. (2013). Atlantic Hurricane Database Uncertainty and Presentation of a New Database Format. *Monthly Weather Review*, *141*(10), 3576–3592. https://doi.org/10.1175/MWR-D-12-00254.1

Examination of Similarity, Difference and Deficiency of Gauge, Radar and Satellite Precipitation Measuring Uncertainties for Extreme Events Using Conventional Metrics and Multiplicative Triple Collocation. *Remote Sensing*, *12*(8), Article 8. https://doi.org/10.3390/rs12081258
Mazza, E., & Chen, S. S. (2023). Tropical Cyclone Rainfall Climatology, Extremes, and Flooding Potential from Remote Sensing and Reanalysis Datasets over the Continental United States. *Journal of Hydrometeorology*, *24*(9), 1549–1562. https://doi.org/10.1175/JHM-D-22-0199.1

Li, Z., Chen, M., Gao, S., Hong, Z., Tang, G., Wen, Y., Gourley, J. J., & Hong, Y. (2020). Cross-

Medlin, J. M., Kimball, S. K., & Blackwell, K. G. (2007). Radar and Rain Gauge Analysis of the Extreme Rainfall during Hurricane Danny's (1997) Landfall. *Monthly Weather Review*, *135*(5), 1869–1888. https://doi.org/10.1175/MWR3368.1

Necker, T., Wolfgruber, L., Kugler, L., Weissmann, M., Dorninger, M., & Serafin, S. (2024). The fractions skill score for ensemble forecast verification. *Quarterly Journal of the Royal Meteorological Society*, *150*(764), 4457–4477. https://doi.org/10.1002/qj.4824

National Oceanic and Atmospheric Administration (NOAA). (2023, June 13). *Z-time* (Coordinated Universal Time) | National Oceanic and Atmospheric Administration. https://www.noaa.gov/jetstream/time

Oldenborgh, G. J. van, Wiel, K. van der, Sebastian, A., Singh, R., Arrighi, J., Otto, F., Haustein, K., Li, S., Vecchi, G., & Cullen, H. (2017). Attribution of extreme rainfall from Hurricane Harvey, August 2017. *Environmental Research Letters*, *12*(12), 124009. https://doi.org/10.1088/1748-9326/aa9ef2

Rappaport, E. N. (2014). Fatalities in the United States from Atlantic Tropical Cyclones: New Data and Interpretation. https://doi.org/10.1175/BAMS-D-12-00074.1

Reed, K. A., Stansfield, A. M., Wehner, M. F., & Zarzycki, C. M. (2020). Forecasted attribution of the human influence on Hurricane Florence. *Science Advances*, *6*(1), eaaw9253. https://doi.org/10.1126/sciadv.aaw9253

Rickard, L. N., Schuldt, J. P., Eosco, G. M., Scherer, C. W., & Daziano, R. A. (2017). The Proof is in the Picture: The Influence of Imagery and Experience in Perceptions of Hurricane Messaging. *Weather, Climate, and Society*, *9*(3), 471–485. https://doi.org/10.1175/WCAS-D-16-0048.1

Schmidt, J. A. (2007, January 18). *Spatially-variable, physically-derived flash flood guidance*. https://ams.confex.com/ams/87ANNUAL/techprogram/paper_120022.htm

Schott, T., Landsea, C., & Hafele, G. (2012). *The Saffir-Simpson Hurricane Wind Scale*. https://mail.hwn.org/media/pdf/sshws.pdf Senkbeil, J. C., & Sheridan, S. C. (2006). A Postlandfall Hurricane Classification System for the United States. *Journal of Coastal Research*, 22(5 (225)), 1025–1034. https://doi.org/10.2112/05-0532.1

Shepherd, J. M., Grundstein, A., & Mote, T. L. (2007). Quantifying the contribution of tropical cyclones to extreme rainfall along the coastal southeastern United States. *Geophysical Research Letters*, *34*(23). https://doi.org/10.1029/2007GL031694

Song, J. Y., Alipour, A., Moftakhari, H. R., & Moradkhani, H. (2020). Toward a more effective hurricane hazard communication. *Environmental Research Letters*, *15*(6), 064012. https://doi.org/10.1088/1748-9326/ab875f

Stewart, S. R., & Berg, R. (2019). *Hurricane Florence (AL062018)* (National Hurricane Center Tropical Cyclone Report). National Hurricane Center (NHC).

https://www.nhc.noaa.gov/data/tcr/AL062018_Florence.pdf

Swain, D. L., Wing, O. E. J., Bates, P. D., Done, J. M., Johnson, K. A., & Cameron, D. R. (2020). Increased Flood Exposure Due to Climate Change and Population Growth in the United States. *Earth's Future*, 8(11), e2020EF001778. https://doi.org/10.1029/2020EF001778

Vallee, D. (2022). Updating Excessive Rainfall Outlook Probability Definitions on or about Thursday February 10, 2022. National Weather Service.

https://www.weather.gov/media/notification/pdf2/scn22-

18 updating ero probability definitions.pdf

Weather Prediction Center (WPC). (2024, March 6). *Product Information*. WPC Product Information. https://www.wpc.ncep.noaa.gov/html/fam2.shtml

Wehner, M. F., & Kossin, J. P. (2024). The growing inadequacy of an open-ended Saffir—Simpson hurricane wind scale in a warming world. *Proceedings of the National Academy of Sciences*, 121(7), e2308901121. https://doi.org/10.1073/pnas.2308901121

Xie, P., Chen, M., Yang, S., Yatagai, A., Hayasaka, T., Fukushima, Y., & Liu, C. (2007). A Gauge-Based Analysis of Daily Precipitation over East Asia. *Journal of Hydrometeorology*, 8(3), 607–626. https://doi.org/10.1175/JHM583.1

Zhao, B., & Zhang, B. (2018). Assessing Hourly Precipitation Forecast Skill with the Fractions Skill Score. *Journal of Meteorological Research*, 32(1), 135–145.

https://doi.org/10.1007/s13351-018-7058-1